International Journal of Material Forming (2022) 15: 39
https://doi.org/10.1007/s12289-022-01682-8

ESAFORM 25 YEARS ON

Advances in composite forming through 25 years of ESAFORM

Philippe Boisse[1] · Remko Akkerman[2] · Pierpaolo Carlone[3] · Luise Kärger[4] · Stepan V. Lomov[5] · James A. Sherwood[6]

Received: 23 December 2021 / Accepted: 15 March 2022 / Published online: 20 April 2022

Abstract

The increase in the number of structural applications of composite materials, especially in the aerospace and automotive industries, has led to a demand for robust models to simulate composite forming processes. The mechanical behaviour of composite materials during forming is relatively complex due to their fibre-matrix composition. Many research studies have been conducted in the past 25-plus years into experimental methods for the characterization of the mechanical behaviours that are exhibited by textile-reinforced composite material systems during forming and into the development of material models to be used in computer codes for forming simulations. These studies have been presented and discussed in the ESAFORM conferences since 1997 and especially in the 'Composite Forming Processes' mini-symposium launched in 2001. This article presents a survey of the research carried out in this context. Mechanical characterization tests specific to composite forming are presented as well as recent analysis techniques such as digital image correlation and X-ray tomography. Three-dimensional mechanical behaviour laws, in particular hypo- and hyperelastic, have been developed and extended to second gradient models. Specific shell approaches have been presented and their application to wrinkling analysis. Resin flow and permeability analysis is another area of research in composite forming processes which are discussed in this article. Research on certain processes is also presented, in particular thermoforming of thermoplastic composites, wet compression moulding, pultrusion, automated fibre placement and three-dimensional printing. This comprehensive review of the works of multiple research groups is a recognition of the breadth and depth of efforts that have been invested into the understanding of the manufacturability of textile-reinforced composite materials.

Keywords Composites · Forming · Fibre · Matrix

Introduction

When the mechanical characteristics/mass ratio is important, composite materials have become the material of choice. The transportation industry has been steadily increasing the penetration of composites to reap the benefits of reduced fuel costs and increased range of operation. For example, in civil aviation, the two most recent long-range aircraft, the Airbus A350 and the Boeing 787, have made extensive use of composites in the airframe. The manufacture of composite parts frequently requires forming operations, and these forming processes can be challenging when considering the very particular mechanical behaviors of a given composite material system during its deformation.

Since 2001, the "composite forming process" mini-symposium of the annual ESAFORM conference has brought together researchers from across Europe and around the world to present their work and discuss the analysis and simulation of composite forming. More than 500 presentations

✉ Philippe Boisse
philippe.boisse@insa-lyon.fr

1 Université de Lyon, LaMCoS, CNRS, INSA Lyon, 69621 Villeurbanne, France

2 University of Twente, Drienerlolaan 5, 7522NB Enschede, the Netherlands

3 Department of Industrial Engineering, University of Salerno, 84084 Fisciano, SA, Italy

4 Institute of Vehicle System Technology, Karlsruhe Institute of Technology, Karlsruhe, Germany

5 Department of Materials Engineering, KU Leuven, Leuven, Belgium

6 Department of Mechanical Engineering, University of Massachusetts Lowell, Lowell, MA 01854, USA

in 20 conference proceedings have been realized through this international collaboration. This symposium has been a significant venue for the sharing of innovations and collaborations on this very important scientific and technical topic. The purpose of this article is to present an overall summary of the main topics that have been addressed at these annual ESAFORM conferences and to highlight some of the progress that has been made during these two decades. The main composite manufacturing processes that have been presented at these conferences are considered in the present paper.

The analysis and modeling of the deformation behaviors of composite textile reinforcements and prepregs can be performed at one or more of three scales: (1) at the fibre scale (microscopic), (2) at the yarn scale (mesoscopic) and/or (3) at the whole preform scale (macroscopic). The models and simulations presented in this paper are done at the macroscopic scale which is the most widely used for composite forming analyses of whole structural parts.

The fibrous composition of the textile reinforcements and prepregs leads to a very specific mechanical behavior during shaping. In-plane shear, i.e. trellising, is the mode of deformation for a woven textile to conform double-curvature geometries. Its study constitutes an important topic of the field. From an experimental point of view, the analysis of in-plane shear uses mainly two tests: the "picture frame test" and the "bias extension test" which are specific to textile reinforcements. A benchmark has been initiated in the framework of the ESAFORM conferences and carried out by seven international research teams. The bending stiffness of textile reinforcements is much lower than that of continuous materials due to the relative sliding of the fibres. Thus, the standard bending theories of solids do not apply. Specific tests for textile bending needed to be developed and evaluated. The compaction behavior of a fibrous reinforcement is important because this deformation makes it possible to evacuate the voids during the impregnation and consolidation phases and to fix the fibre content of the preform. Optical methods have been extensively developed over the last twenty years to analyze the geometry and deformation of composites during forming. In particular, digital image correlation allows analysis of flat or non-planar surfaces and X-ray tomography gives the geometry inside the fibrous reinforcements. The specificities of the mechanical behavior of non-crimp fabrics which are interesting for industrial applications, such a wind turbine blades, are another textile architecture that is a subject of research and likewise in need of using the aforementioned methods to characterize their mechanical behaviors.

Three-dimensional behavior laws must be written in the framework of geometric nonlinearities with strong anisotropy in a reference frame of that evolves with the deformation. Hypoelastic and hyperelastic laws have been proposed for textile reinforcements. The laws written in the Cauchy framework are not always sufficient and second gradient laws have been proposed. Textile composites reinforcements are generally thin and forming simulations use finite element shells. These are very specific considering the bending behavior with low stiffness and does not follow the classical models. Compaction is an important aspect, and developments are currently in progress for solid-shell finite elements which model this transverse compression. Wrinkling during draping is one of the main defects that can develop during this process. Their simulation is an element that makes it possible to determine the processing conditions to avoid them. Thermoforming of thermoplastic prepregs provides a rapid manufacturing process for composite parts. In this case, the modeling must consider the thermo-mechanical coupling and the viscous character of the mechanical behavior.

In Liquid Composite Molding (LCM), the resin is injected into a preform. The analysis and simulation of this injection is a wide field of research. In particular, the determination of the permeability of the textile preform, which represents its ability to allow the resin flow, is the subject of numerous studies and has given rise to several international benchmarks. The analysis, modeling and simulation of the different aspects of LCM processes and in particular of the mold flow are the subject of numerous works.

In addition to LCM processes and thermoforming of prepregs, other composite manufacturing processes are emerging. Automated fibre placement and robotic layup are widely used in the aerospace industry. To produce complex shaped parts without using a mold, additive manufacturing is an emerging technology for the manufacture of fibre-reinforced composite parts. Pultrusion is an efficient but complex process that produces composite profiles with a constant cross-section.

Section 2 'Materials characterization' of this paper presents the specificities of the main deformation modes of composite textile reinforcements in particular in-plane shear, bending and compaction and also the mechanical behavior of Non-Crimp Fabrics (NCF) and the techniques of analysis by digital image correlation and micro-computed tomography. Section 3 'Constitutive models for composite forming' deals with three-dimensional constitutive models adapted to textile reinforcements. The simulation of composite reinforcement forming processes is discussed in Section 4 'Composite reinforcements forming simulation'. The simulation of continuous fibre-reinforced thermoplastics thermoforming is also analysed in this section. Section 5 'Resin infusion, permeability' concerns the injection of the resin into the fibrous reinforcements and the analysis of the permeability. In Section 6, 'Alternative manufacturing processes' processes such as automated fibre placement, three-dimensional printing, wet compression moulding and pultrusion are discussed.

Materials characterization

Materials characterization: In-plane shear

Composite forming and in-plane shear

Draping a textile composite reinforcement or prepreg over a double-curvature surface requires membrane deformation of the reinforcement. As the fibers are quasi-inextensible in a textile reinforcement, a textile conforms to the surface by in-plane shear deformation (Fig. 1a), i.e. trellising of the tows. The angles required for forming can become large, and there is a forming limit, known as the locking angle, as a function of the textile achitecture. In the case of thermoset or thermoplastic prepregs, the matrix is present but is soft enough during forming so that the prepreg can deform. Because in-plane shear is the primary mode of deformation during draping, it has been extensively studied, and in particular at the ESAFORM conferences. Lindberg [1], Grosberg [2] and Kawabata [3] carried out the first works concerning in-plane shear in the sixties/seventies. Studies concerning the in-plane shear behaviour of textile reinforcements have become numerous with the development of modeling of composite forming [4, 5].

Experimental tests: Picture frame test and bias extension test

Two main tests have been developed to analyse the in-plane shear behaviour of textiles. The picture frame test is composed of four rigid and articulated bars of equal length (Fig. 1b), i.e. a four-bar linkage. When the initially square geometry becomes a lozenge, i.e. diamond shape, the specimen inside the frame is assumed to be subjected to a pure and uniform in-plane shear (at least in theory). This assumption also requires no slippage between the warp and weft yarns. The bias-extension test is a tensile test that is performed on a rectangular specimen where the yarns are initially oriented at ± 45° (Fig. 1c). During the 2000s, many studies have been carried out on the analysis of these tests, in particular the determination of the equations relating the forces on the machine to the shear stresses in the specimen [6–10] and in Digital Image Correlation for the characterization of the strain field and assessment of its homogeneity (see Section 2.5 on Digital Image Correlation (DIC)).

Both the picture frame and bias-extension tests have the objective to characterize the in-plane shear behaviour of a textile reinforcement; however, they are technically different and present some test-specific benefits and challenges. The picture frame test is kinematically highly constrained. All the edges of the specimen are blocked on the frame, and care must be taken to avoid tensions in the fibers which can disturb the test. In the bias-extension test, the fibers have at least one free end, which avoids parasitic tensions; however, the shear kinematics rely on assumptions, in particular the non-slip of the warp and weft yarns. For some reinforcements, this assumption can be difficult to verify. Studies have been made to compare these two tests [6, 11, 12].

Shear tests at high temperature

The forming of thermoset and thermoplastic prepregs are performed at elevated temperature. In the case of thermoset

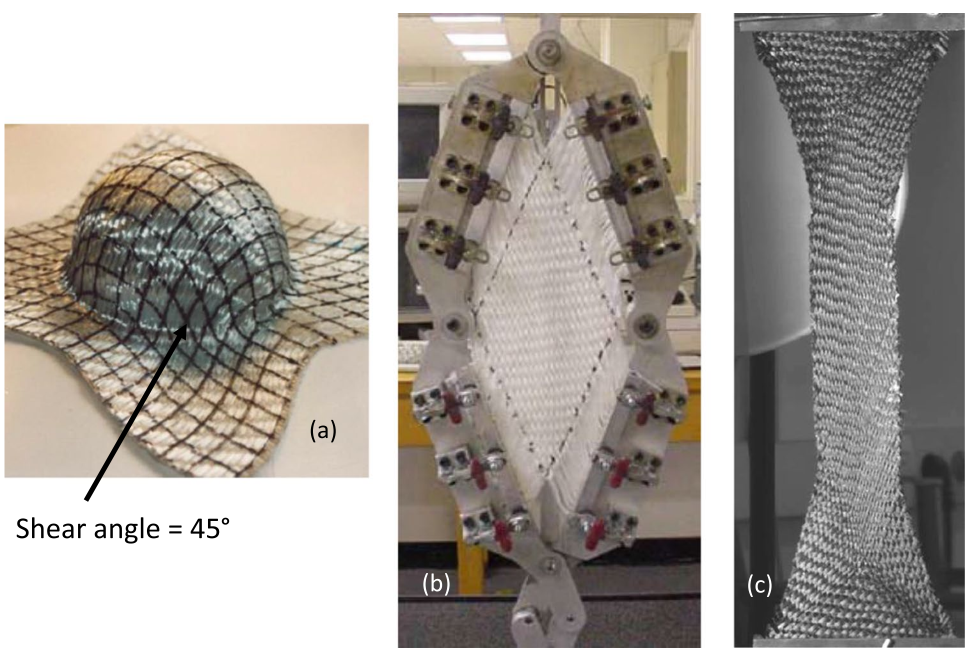

Fig. 1 (**a**) In-plane shear in forming [28], (**b**) Picture frame test [29], (c) Bias-extension test [28]

prepregs, forming takes place before curing. In the case of thermoplastic prepregs, forming occurs at a temperature above the melting point. The shear properties are typically temperature-dependent, and thus these properties must be determined for all temperatures that can occur during thermoforming. In-plane shear tests are performed at different temperatures in thermal chambers [4, 6, 11, 13–15]. These tests can be challenging in particular the need to achieve homogeneity of the temperature. In-plane shear tests can be performed at different speeds to measure the influence of strain rate. The effect of the strain rate has been observed by some to be less important than the effect of the temperature [13].

Influence of the tensions in the yarns

In-plane shear stiffness is increased when a textile reinforcement is subjected to tension. Studies have analysed this phenomenon [7, 12, 16–18] and have shown that the influence of these tensions is important, especially with regard to the development of wrinkles [19]. An advantage of the bias-extension test is that the yarns have at least one free end and are subjected to insignificant low tensions during the test. To analyse the tension-shear coupling, a biaxial bias-extension test was developed [20], and modifications of the picture frame tests, coupled with tension [21–23].

The locking angle and its limitations

During a picture frame test, wrinkles appear from an angle called "shear locking angle" [24–26]. This angle is used by some simulation approaches of draping processes as a limit above which wrinkling of the textile reinforcement appears. As shear angles become large, in-plane shear stiffness increases and this is indeed a factor favourable to the development of wrinkles. However, the development of wrinkles involves all the stresses and stiffnesses, and it is difficult to conclude whether wrinkles occur with the plane shear angle only. Very large shear angles ($>60°$) have been measured when using a high binder pressure without wrinkles appearing [19, 27].

A benchmark on in-plane shear behavior of woven fabrics

To bring together the results obtained by different teams on in-plane shear behaviour, a benchmark was launched at the initiative of Jian Cao and Julie Chen [9, 30]. It gave rise to presentations and discussions at the 2001 NSF Composite Sheet Forming workshop and at the ESAFORM conferences from 2004 to 2007. Three different commingled fiberglass-polypropylene woven fabrics (donated by Vetrotex Saint-Gobain) were provided to the seven research groups: Northwestern University in the USA, University of Massachusetts Lowell in the USA, University of Twente in the Netherlands, University of Nottingham in UK, Katholieke Universiteit Leuven in Belgium, Hong Kong University of Science and Technology in Hong Kong, and Institut National des Sciences Appliquées of Lyon in France. The experimental tests were carried out with the picture frame test and the bias-extension test. The geometry of the different devices, the procedures used by the different teams and results were analysed, and rules of good practice were established. A major issue was to synthesize the relationships to determine the shear force versus shear angle.

Bending of composite reinforcements

Textile composite reinforcements and prepregs have a low bending stiffness due to their fibrous composition. Membrane approaches have been proposed to simulate their deformation [31–34]. Nevertheless, it has been shown that the bending stiffness plays a role in this deformation, in particular with respect to the development of wrinkles during forming and the shape of these wrinkles [35–38]. Consequently, it is necessary to account for bending in the simulation of draping processes. The analysis of textile bending is complex because it cannot be modeled by standard bending approaches. In the case of classical continuous materials, e.g. metals, the standard plate and shell theories of Kirchhoff and Mindlin have been developed. In these theories, the membrane and bending stiffnesses are interdependent and the bending stiffness is given by the tension stiffness and the thickness. This approach is not applicable to fibrous reinforcements and would lead to a very overestimated bending stiffness. It can be seen in Fig. 2a that the material normals are not perpendicular to the mean surface in the case of a textile reinforcement contrary to the case of a classical material which follows the Kirchhoff theory (Fig. 2b). The slippage between the fibres of a textile is the cause of the low bending stiffness. This property plays a major role in the draping of reinforced textile composites. The tension and bending stiffnesses are coupled in the case of Kirchhoff's theory, but they are often assumed to be "decoupled" for fibrous materials [39, 40].

Experimental analyses of textile reinforcement bending property

Because the bending behavior of textile reinforcements cannot be deduced from the tensile behavior as is done for monolithic materials, experimental characterization of the bending behavior is necessary. Different methods have been proposed for this experimental characterization. Pierce's method [41] uses the cantilever bending of a textile specimen subjected to its own weight (Fig. 3a). The deflection of the fabric can be used to calculate the

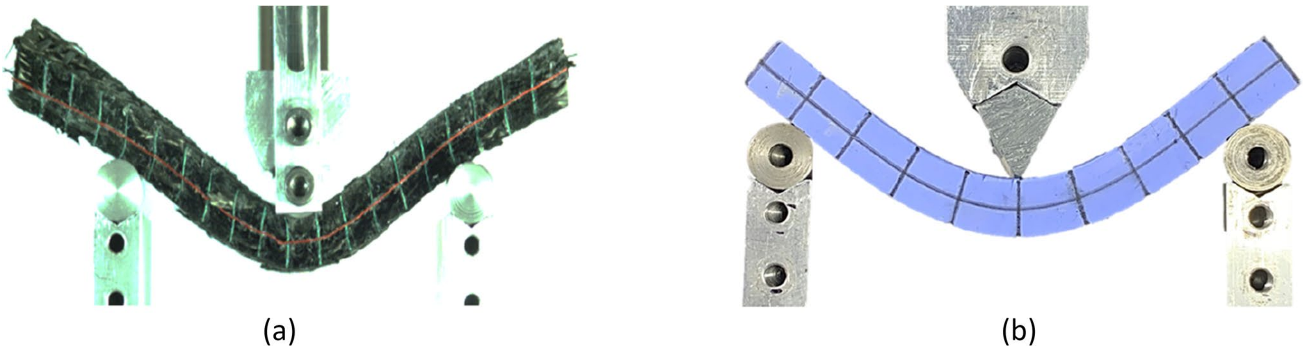

Fig. 2 **a** Bending of a fibrous material. **b** Bending of a classical continuous material [55]

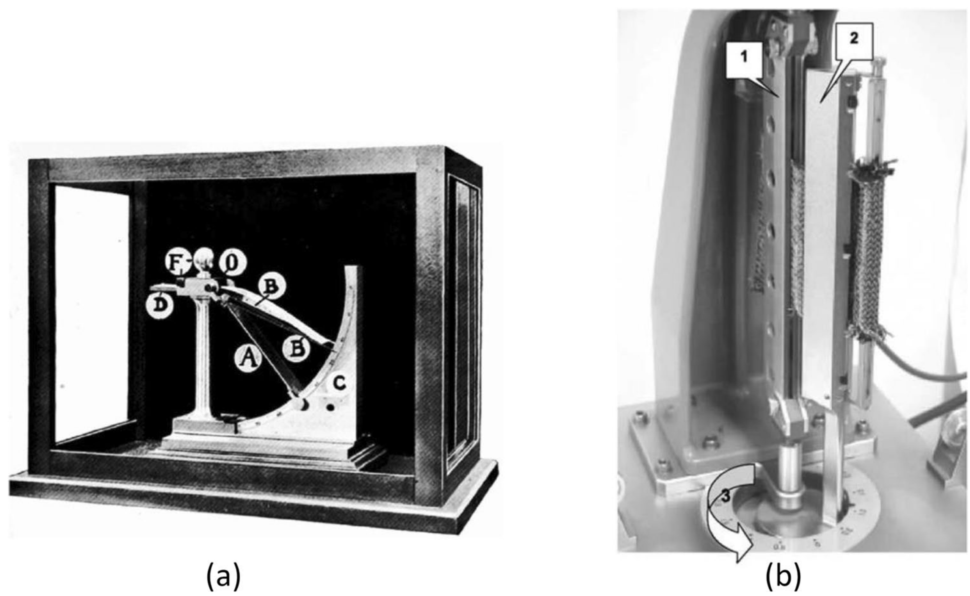

Fig. 3 **a** Peirce flexometer [41], **b** Kawabata bending test—KES-FB2 [47]

bending stiffness. If the stiffness is assumed to be constant, it is sufficient to measure the length of the reinforcement necessary for its extremity to come into contact with a plane of fixed inclination (41.5° according to the norm) to determine this stiffness [42]. On the other hand, an optical measurement of the deformed midline makes it possible to calculate the curvature at any point of the specimen, and thus, to identify the possibly nonlinear moment–curvature relationship [43–45]. The Kawabata bending test (KES-F2), imposes the curvature of a specimen whose two ends are clamped in the system (Fig. 3b) [46, 47]. This system allows to set the loading speed and to perform loading cycles. Other devices have been developed on the same principle and used for viscoelasticity analyses [48, 49]. Three-point bending, which is widely used for other materials, is also used for textile reinforcements and prepreg provided that their bending stiffness is sufficiently high [50, 51]. The different setups can be used to test the bending properties as a function of temperature [36, 48, 52–54]. Prepregs are very sensitive to temperature, and care must be taken with respect to initiating cure of the matrix material during the characterization experiment.

Consideration of bending properties in numerical simulations of composite forming

The tests presented in Section 2.2.1 allow the determination of the effective bending stiffness of textile reinforcements; however, the implementation of these properties into the deformation simulations is not a simple task. The classical shell finite elements based on Kirchhoff or Mindlin theories couple the membrane and bending properties, but this coupling does not apply to textile reinforcements. To accommodate the measured bending stiffnesses, it is necessary to set up an approach that decouples the bending and tension stiffnesses. This aspect is presented in Section 4.1 (Shells) and in [39, 40, 56].

Transverse compression

Compression (compaction) of a fibrous reinforcement is an inherent part of the composites forming process due to the nature of bundles of fibres comprising the tows or yarns, where a yarn is a twisted bundle of fibres. It serves two purposes. First, the applied pressure promotes evacuation of voids during the preform impregnation and consolidation phase of production. Second, the preform compaction creates a fibre-volume fraction in the final cured composite, which provides the desired mechanical properties of the part. The phenomenon of the preform compaction in the composite processing differs from the phenomena of compaction in textile technology mainly by the level of the applied pressure. The latter is related to the fabric handling and deals with pressure up to ~ 1 kPa (see (2008)). In the composites processing, the pressure ranges from ~ 0.1 MPa (1 bar, vacuum pressure) to ~ 1 MPa (autoclave) up to ~ 10 MPa (compression moulding).

The main question which should be answered by the experimental or modelling description of the preform compaction is: "What is the pressure needed to reach the required fibre volume fraction (or the given thickness)?", or: "What is the fibre volume fraction created by the given pressure?". The former is relevant for processes in a closed mould (RTM, compression moulding), the latter for open mould processing (vacuum infusion, autoclave processing, thermoforming).

The compaction behaviour of composite reinforcements has been studied extensively in 1990s – 2010s, see, for example [57–59] and is well understood. A typical pressure vs. thickness diagram has two regions: the first (low pressure) is controlled by change of the fibre crimp, and the low compression resistance is given by low bending stiffness of the fibres; in the second (high pressure, from ~ 0.05 MPa) the fibres come close together, the number of contacts between them increases dramatically, there is no more freedom for the fibres to bend, and the resistance to compression is more defined by high Hertzian contact forces than by bending of the fibres. Different textile and non-woven materials were investigated, including 3D textiles [60], and nano-engineered textiles [61, 62]. Descriptive and predictive models for the pressure – thickness relation are proposed [63–67]. Apart from the dry compaction, the wet compaction and viscoelasticity of the (pre)-impregnated preforms has been studied [68, 69].

In 2019, a benchmark study of fibrous reinforcement compressibility was started. The benchmark studied two types of glass-fibre fabrics (woven and NCF), with 26 participating labs, both in dry and wet compaction [70]. The benchmark has revealed a high variability of the compression test. For the data from all participants, coefficients of variation of maximum recorded pressure for a fixed final preform thickness were up to 50%. Three main sources of variability were identified: thickness measurement, approach to compliance correction and parallelism, and specimen saturation in wet compression tests. Figure 4 illustrates a typical compression test configuration and the obtained compression curves.

Stemming from the benchmark, research of new aspects of the preform compression have started: development of reference specimens for the compression test [71], machine compliance during the test [72], viscoelasticity during compaction [73]. The second benchmark, which aims at normalisation of the measurements, is expected to start in 2021 – 2022.

Specific deformability of stitched NCF

Non-crimp fabrics (NCF), which can include "multi-axial multi-ply warp-knitted preforms", are special among textile composite reinforcements because of their lack of waviness that is seen in a woven textile. The fibres in NCFs are arranged in unidirectional plies and are essentially straight, with small distortions created by the stitching (Fig. 5). These distortions are sites for the development of resin-rich zones near the stitching sites, which play an important role in impregnation of the fabric. Deformability of NCFs, hence their behavior in forming, is strongly affected by the stitching, which creates low extensible connections, limiting shear and tension compliance in certain directions [74]. Most popular carbon fibre NCFs, used in automotive and aeronautic industries are multiaxial. The reinforcement for wind turbine blades is primarily unidirectional glass fibre NCFs in combination with ± 45° cross-ply NCFS for torsional stiffness. The book [75] gives an overview of the NCF-related work in 1990s and 2000s. Since then, the research in NCF internal structure and formability was focused on in-depth investigation of the two effects mentioned above: fibre distortion in the plies and the effect of the stitching on deformability and drape. This research was particularly intense during the 2015–2021 period.

The internal structure on NCFs is being studied under high-resolution, high-fidelity instruments such as scanning electron microscopy [76] and micro-CT [77–79]. For unidirectional glass NCFs, this work resulted in reliable characterization of the fibre waviness, which influences mechanical performance [80–83]. Multi-scale, multi-step description of the orientation variability was applied to multi-axial NCFs [84].

A continued work on the deformability characterization [85–92] creates a comprehensive database to be used in the forming simulations. This work also includes specific problems as fabric-tool friction characterization [93], localization of transverse tension [86], superposition of transverse tension and shear [94], difficulties in assessing the strain

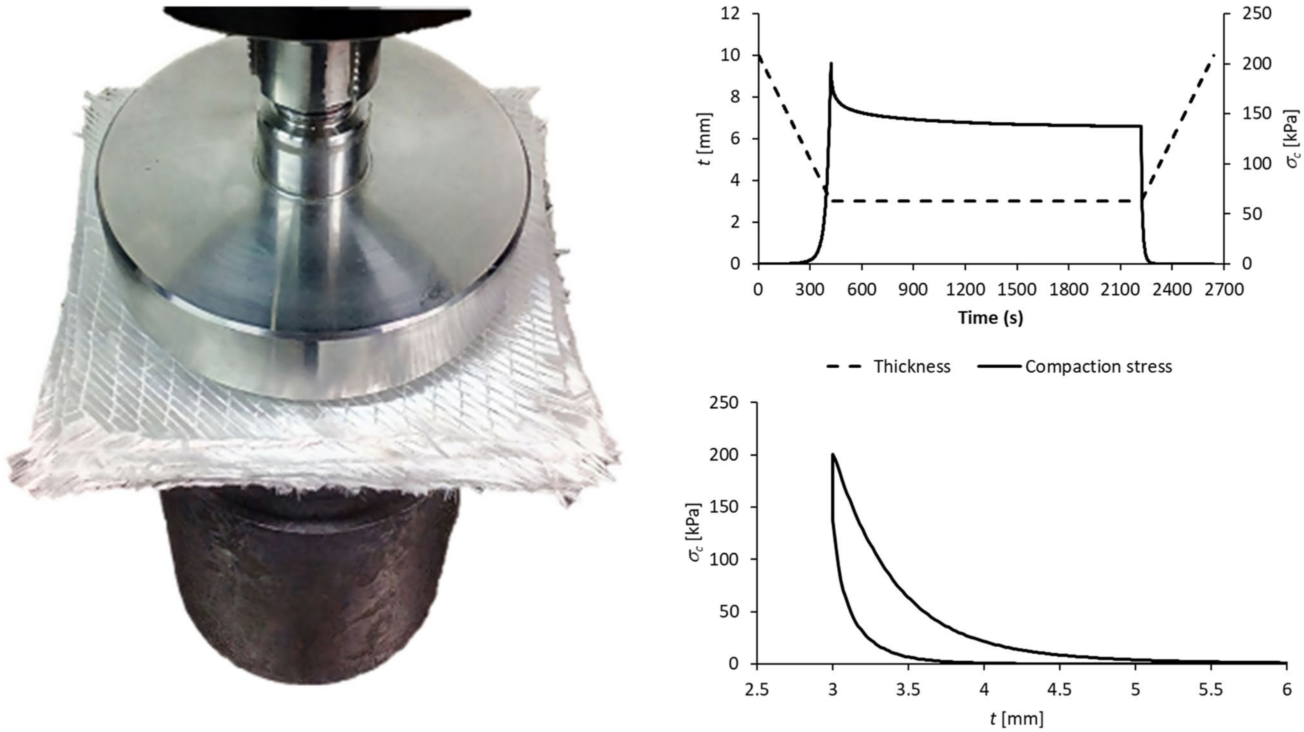

Fig. 4 Compaction tests of textile reinforcements: (**a**) a typical test configuration [72], (**b**) thickness – time and compression stress – thickness diagrams of the test [70]

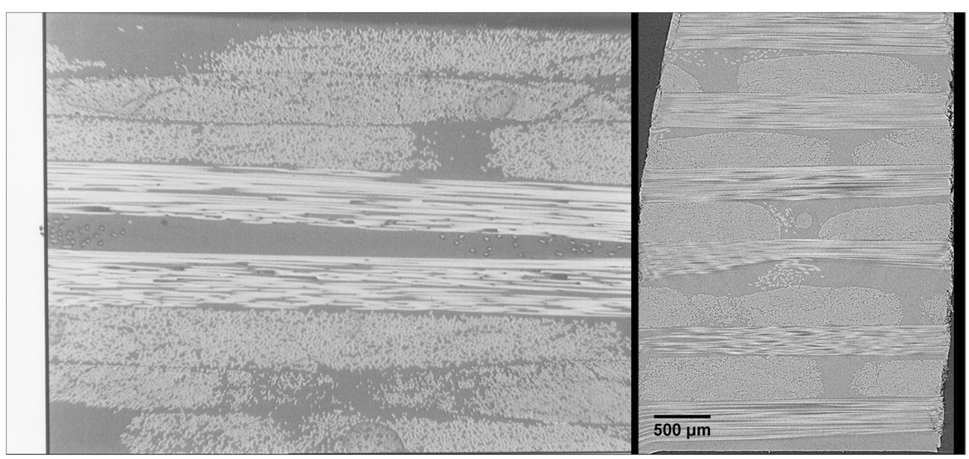

Fig. 5 Internal structure of carbon fibre/epoxy NCF composite laminates: quasi-isotropic $[90°/-45°/45°/0°]_s$ (left) and cross-ply $[90°/ 0°]_8$ [75, 77]

fields via DIC, caused by the fabric surface distortion [95], compaction characterization [96], forming of NCF composites with continuous NCFs [97]. The special attention is on wrinkling and other local defects of draping [98–101] and its predictability during forming on part level [102]. Deformability of thermoplastic NCF sheets was studied in near-processing conditions in temperature and strain rate [103].

In the testing for formability, apart from the research techniques, automated, industrial-lab-suited devices appear: a Drape-test device, which was applied to investigations of NCF formability [104], robot-based optical measurement [105], as well as quality assessment methods for the draping [106, 107].

Understanding of the draping mechanics of NCFs has led to industrial developments: a draping unit, for balancing fabric tension and consolidating continuously across the layup width, accounting for shearing of the previously laid fabric [108], automated draping methods for layup of NCFs for wind turbine blades [109], flexible clamping methods [110], design of the stitching based on the draping requirements [111], identification of the forming limits for NCFs [112].

Digital image correlation and micro-computed tomography

Since the first applications of Digital Image Correlation (DIC) to study full-field strain fields in dry textiles, notably appeared first in ESAFORM Proceedings [113–117] and then published in journals [118–121], DIC has since become a common method for extensometry during mechanical tests on dry textiles and for measuring reinforcement local strains during draping. For the former (mechanical testing) DIC was used for picture frame, bias-extension and bi-axial tension [12, 15, 85, 118, 122, 123] to name a few. For the latter, 3D DIC provides strain fields of the draped reinforcements, allowing identification of regions with a dangerously high shear or local yarn-level defects [56, 94, 124–128], Fig. 6. The literature which reports the results of mechanical tests and draping of dry reinforcements using DIC is too extensive to cover it here. However, the choice of DIC parameters for dry textiles tests is still more an art than a precise science, and a benchmark exercise could be a good way towards normalisation of such measurements.

Micro-computed X-ray tomography (μCT) is applied for studies of textile internal structure since 2000s [129–132]. In the last decade it has become a widely used technique, applied to glass, carbon and natural fibre reinforcements of different textile architecture [131, 133–137]. Figure 6b shows an example of μCT image of a 3D woven reinforcement. Recent reviews [138, 139] can serve as an entry to the field.

The attainable resolution of μCT images is down to 1 μm and lower, with the image size of few centimetres. This level of detail makes it possible to obtain good quality images of textile unit cells and effective segmentation of the image for the reconstruction of the yarn volumes and paths, with subsequent transformation into a finite elements (FE) model [135, 140–142].

μCT has been used for validation of the predictions of details of the reinforcement deformation on the yarns level [131, 143] and detailed studies of the deformed 3D reinforcement architecture [136].

Apart from FE modelling, a μCT image allows quantification, which gives general characterisation of uncertainties of the fibrous structure [144], as fibre and yarn misalignments and deviations of the yarn paths [145, 146]. Such quantification does not necessarily use resources-intensive image segmentation, which requires high image resolution: it can use, for example, structure tensor methods [147], which are fast, effective and well-compared with the high-fidelity segmentation [148].

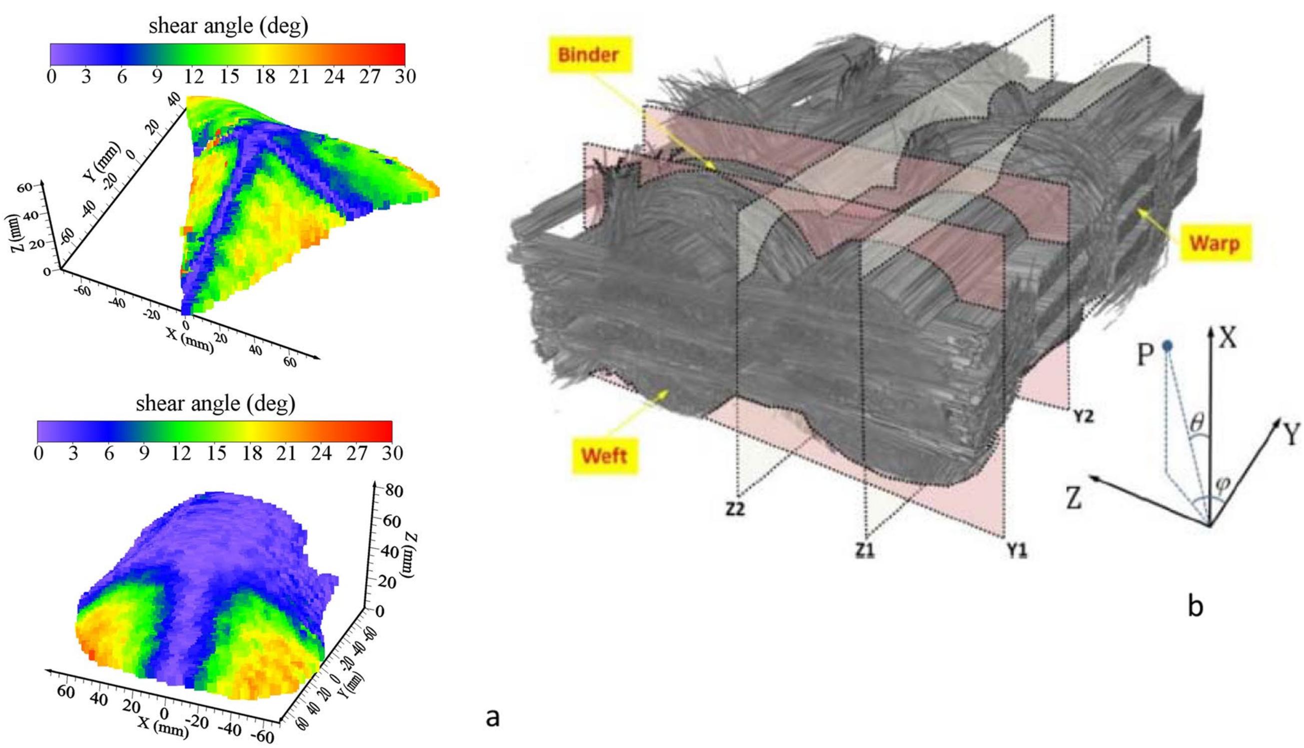

Fig. 6 **a** DIC-registered distributions of the shear angle on the surface of a 3D woven fabric, draped over tetrahedron and double-dome moulds [127]; **b** micro-CT of a 3D woven fabric [133]

Constitutive models for composite forming

Simulations of the deformation of textile reinforcements can be performed at the micro-, meso- or macro-scale. The description of the internal structure of the fibrous reinforcement is more detailed at the micro-scale and, to some extent, at the meso-scale than what can be derived at the macro-scale. However, to perform simulations of the forming process on either the micro- or meso-scale is relatively expensive in computational resources and time. As a result, draping simulations of textile reinforcements are typically performed at the macroscopic scale for numerical efficiency [149]. At this scale, the constitutive law used in the modeling must reflect the main specificities of the mechanical behavior of fibrous reinforcements. That is, it will be necessary to consider the anisotropy of the behavior in the warp and weft frame which evolves during the transformation because of the in-plane shear. The constitutive model must be written in the framework of geometrical nonlinearities considering large displacements and large shear angles. It must account for the quasi-inextensibility of the fibres and for the in-plane shear behavior, which is strongly nonlinear (Section 2.1). The constitutive model in large deformations can be hypoelastic (law in rates), elastic or hyperelastic (the stresses derive from a strain energy potential).

Hypoelastic models

The explicit dynamics framework that is generally used, in particular in commercial software, computes a stress increment from a strain increment at each time step and is naturally adapted to a hypoelastic approach [150–152]. So-called "non-orthogonal" constitutive models have been proposed for the membrane behavior of woven reinforcements [152, 153] and NCFs [154]. At a given moment of the deformation, these laws use the current position of the warp and weft yarns to express elastic tensile and in-plane shear behaviors. As the main hypoelastic laws use orthogonal rotating frames, an approach proposed in [55, 155, 156] uses two orthogonal frames based on the respective directions of the warp yarns and weft yarns (Fig. 7a).

Hyperelastic models

In hyperelastic models, strain energy potentials are defined to describe the nonlinear behavior of textile composite reinforcements or prepregs. For an initially orthotropic material with two preferred directions (warp and weft) and one direction through the thickness, the potentials depend on invariants of the deformations and these directions [157, 158]. A set of equivalent invariants but concerning each deformation mode can be used to define potentials specific to each deformation mode [159–162]. These hyperelastic approaches are both based on solid foundations and allow, by the choice of the potentials, to define specific and efficient models for a given textile reinforcement. This approach is extended to the hyper-viscoelasticity [163–167]. The potentials corresponding to each deformation mode are generally assumed to be decoupled, but some studies propose models with coupling [168].

Second gradient approaches

The continuum models introduced in Section 3.1 and 3.2 are models of Cauchy. These models are based on the first

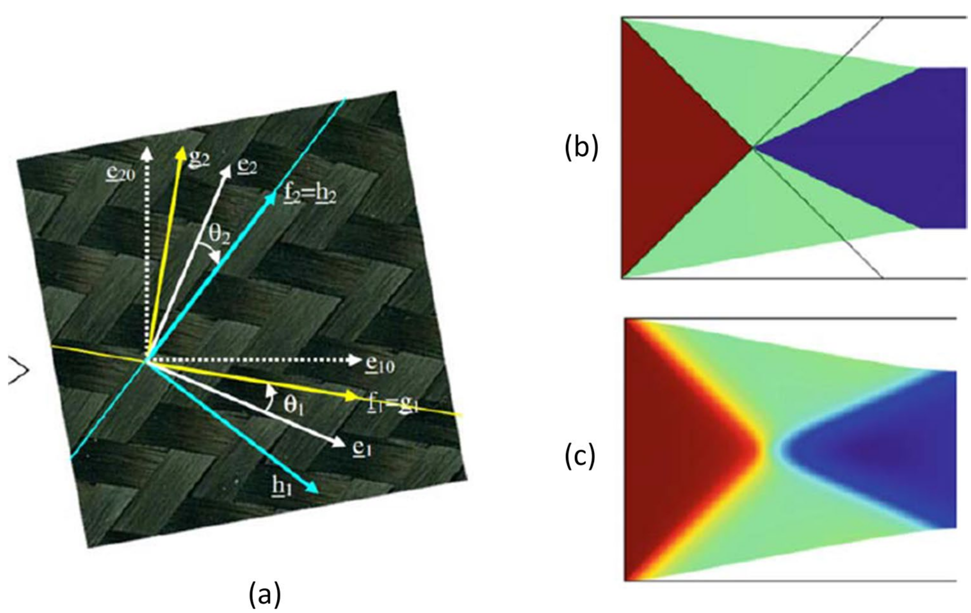

Fig. 7 **a** Fibre frames for a hypoelastic approach [156]. **b** Simulation of the bias-extension test with a first gradient model, **c** with a second gradient model [170]

gradient of displacements. It has been shown that these models have some limitations in the case of fibrous reinforcements [169, 170]. For example, the simulation, using 3D elements and a hyperelastic model, of the three-point bending of a thick reinforcement shown in Fig. 2a leads to parts outside the supports that are not sufficiently raised. The simulation of a bias-extension test by a first gradient model (Fig. 7b) gives a deformation without a transition layer between the different shear zones [169]. In addition, parasitic wrinkles can appear in simulations with 3D elements and a hyperelastic model [171]. These difficulties arise from the inability of a first gradient model to capture the very low transverse shear (given the fibrous composition) and simultaneously to account for the bending stiffness of each fibre [170]. To overcome this difficulty, hyperelastic second gradient models have been introduced. In addition to the potentials based on the displacement gradients, terms based on their second gradient, i.e. on the strain gradients, have been introduced for the shear strain energy potentials [169, 172–175]. The problems highlighted when a Cauchy model is used are solved by this second gradient approach. For example, Fig. 7c shows that in the simulation of a bias-extension test, the transition zones are well described. An alternative to the introduction of second gradient terms in the strain energy potential, is to add to the first gradient potentials, a strain energy related to the curvature of the fibres. This curvature calculation can be done using the position of neighboring elements which is more efficient than the second gradient calculation. The efficiency of this approach is shown in [170, 171]. This approach has been extended to account for the bending stiffness in the finite element plane of shells [176]. This in-plane stiffness is not considered in standard shell elements.

Composite reinforcements forming simulation

The manufacturing processes of composites are numerous and often complex. Simulation of the processes avoids long and expensive developments by trial and error. The simulation of the forming of continuous fiber dry preforms and prepregs is the subject of this section. The simulation of resin injection on fibrous reinforcements is discussed in Section 5.

Shells and solid shells—Macroscopic approaches accounting for membrane and bending behaviour

Forming simulations of dry textiles and prepreg materials require the characterization and modelling of their mechanical behaviour. Early approaches utilised a membrane hypothesis, neglecting the material bending stiffness [32, 177–181]. It has been shown, however, that the formation of wrinkles and other forming effects requires the consideration of the reinforcement's bending stiffness [35, 39, 56], which has to be considered decoupled from the membrane behaviour [35, 54, 125, 182]. Therefore, conventional shell theories are not applicable and superimposed membrane and shell elements [40, 54, 94] or dedicated shell formulations [167, 182–184] are often used. The shell element approaches for macroscopic forming simulations can be divided in two categories, semi-discrete approaches and continuous approaches.

Under the category of semi-discrete approaches, a class of three-noded shell elements have been developed based on the work of Hamila and Boisse [183]. This category represents an intermediate approach between mesoscopic and continuous approaches. It is based on a decomposition of an element into unit cells according to the main deformation mechanisms during forming. The internal virtual work is accordingly separated into a tension, a shear and a bending part [36, 125, 183, 185]. These approaches were applied to various kinds of reinforcements like woven textiles [125, 186, 187], unbalanced fabrics [35], biaxial NCF [188], and thermoplastic prepregs [36, 185]. The model has been extended by Steer et al. [176] to account for in-plane bending in woven fabrics.

Continuous shell approaches model the membrane and the bending behaviour by separate constitutive equations, which are then combined within one shell formulation. Döbrich et al. [39] proposed a shell-integrated method for membrane-bending decoupling based on laminate theory for biaxial NCF. This approach was later extended by Hübner et al. [189] for 3D-woven fabrics. Dörr et al. [167, 190] developed a three-node Discrete Kirchhoff Triangle (DKT) shell element formulation to model the viscoelastic membrane and bending behaviour of thermoplastic UD-tapes. Liang et al. [184] and Bai et al. [191, 192] proposed shell elements based on Ahmad's approach [193] to model the bending behaviour of fibrous media. The hypotheses of Kirchoff and Mindlin are not applied. The virtual work of the internal forces is modified so that the inextensibility of the fibres is assumed and the slip between the fibres is possible. This approach allows simulations of fibre reinforcement deformation where the material normal agrees with the experiment [192].

Three-dimensional continuous approaches are required to consider effects in the transverse direction, such as compaction or consolidation. This three-dimensional continuous approach can be achieved either by shell elements with additional degrees of freedom in the thickness direction or by solid or (locking-reduced) solid-shell elements. Soulat et al. [182] developed a shell element with a degree of freedom for thickness variations. The formulation avoided locking by uncoupling bending and pinching, resulting in a good agreement with reconsolidation experiments. Chen et al. [195]

proposed a similarly extended shell element for woven composite forming, considering tensile, in-plane shear, bending and compressive behaviour. They studied the influence of shear and bending stiffness on the occurrence of wrinkling. In the case of 3D elements, conventional solid elements are unsuitable for the forming simulation of thin textiles due to numerical locking effects. To alleviate locking, so-called solid-shell elements use techniques like selective reduced-integration or modifications to the strain field and have a "shell-like" behaviour for high aspect ratios [194]. Xiong et al. [196] proposed a prismatic solid-shell element with an additional degree of freedom in the element's centre for an improved calculation of transverse normal stresses, in combination with a discrete Kirchhoff assumption of zero transverse shear strains. The element has successfully been applied to the thermoforming of thermoplastic prepregs and its consolidation to remove voids. Schäfer et al. [194] showed numerical studies of hemisphere forming tests to highlight the advantages of a hexahedral solid-shell elements for the forming of continuous reinforcements, see Fig. 8. The approach was extended by a membrane-bending-decoupling to study the influence on wrinkling [197].

Wrinkling during Composite Forming

Among the defects that can occur during the forming of composites, wrinkling is one of the most severe. One of the major objectives of the simulation of composite forming processes is to determine the conditions that avoid wrinkles [35, 99, 180, 198–203]. Wrinkling can occur during the forming of thin metal parts [204, 205]. For fibrous reinforcements, these wrinkles are even more frequent because the fibrous composition of the textile reinforcements makes it possible for fibres to slide between each other and the bending stiffness is greatly reduced.

Influence of the Bending Stiffness

Textile reinforcements in composites usually have a small thickness and can be modeled by shells. The bending stiffness is small given the fibrous composition of the reinforcements. Membrane approaches, without bending stiffness, have been used to simulate the draping of textile fabrics [34, 100]. When membrane elements are used for draping simulation, wrinkles may appear. These wrinkles are nevertheless too small compared to reality due to the lack of bending stiffness of the membranes (Fig. 9a) [35]. Considering the bending stiffness, in addition to the tension and transverse shear stiffness, leads to a deformed shape with larger wrinkles in good agreement with reality (Fig. 9b).

Overall, tensile, in-plane shear and bending stiffnesses play a role in the appearance and development of wrinkles. The tensile stiffness is important and leads to a quasi-inextensibility in the direction of the fibres. The in-plane shear angle required to achieve a double-curved shape is often the cause of wrinkling. The size of the wrinkles is determined by the bending stiffness. Figure 9c shows the wrinkles created by the compression of a rectangular textile reinforcement in the fibre direction in the case of bending stiffnesses of 10, 5 and 1 Nmm^{-1} (from top to bottom). The influence of bending stiffness during a thermoforming of a thermoplastic prepreg is analyzed in [36] and confirms the results of Fig. 9c with a decrease in bending stiffness with increasing temperature.

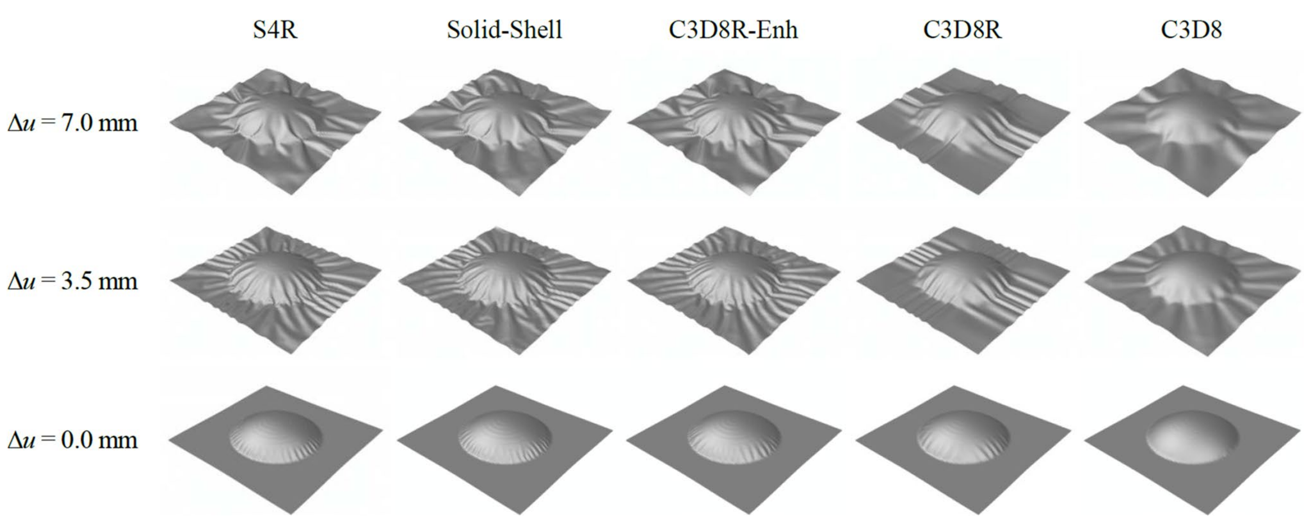

Fig. 8 Hemisphere test | Results for a remaining tool stroke Δu of 7.0 mm, 3.5 mm and 0.0 mm for a conventional shell (S4R), a solid-shell and different commercially available solid elements (C3D8, C3D8R and C3D8R-Enh) [194].

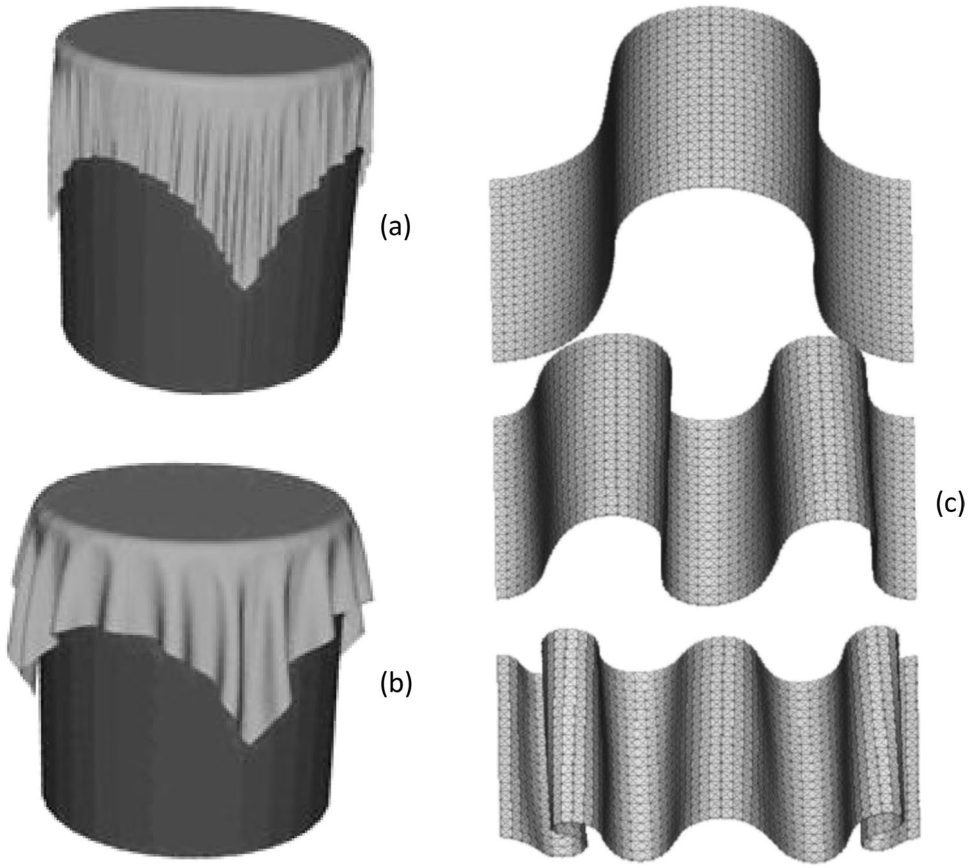

Fig. 9 Simulation of draping on a cylindrical punch. **a** Tensile and in-plane shear stiffnesses. **b** Tensile, in-plane shear and bending stiffnesses. [207] **c** Compression in the yarn direction of a woven reinforcement with different bending stiffnesses [35]

Beyond the Shear Locking Angle

Forming of textile reinforcements on double-curved surfaces is made possible by the low in-plane shear stiffness of the textiles. However, as the shear angle increases, the warp and weft yarns move into contact and the in-plane shear stiffness increases. For a certain shear angle, called the 'Shear Locking Angle', this increase leads to the onset of wrinkles. These wrinkles are clearly visible in a picture frame test [6, 24]. This angle is often considered as a property of the textile and as a value that should not be exceeded during forming to avoid wrinkles [25, 26, 206]. However, the appearance and development of wrinkles is a global phenomenon that involves all the stresses in the textile reinforcement. The determination of the appearance and development of wrinkles requires the simulation of the forming process that accounts for all of the characteristics of the textile reinforcement and the loads during the process. It has been shown in some forming cases that the tensions due to the blank holders can enable forming without wrinkles when the shear angles are much higher than the shear locking angle [27, 35].

Wrinkling in Multi-layered Composites Forming

When forming a stack of textile reinforcement layers, the development of wrinkling is much more likely to occur when the plies have different directions [207–210]. The deformations of plies of different orientations are most likely not going to be the same. This difference in deformations leads to significant slippage between the layers. The resulting friction loads lead to compression zones that create wrinkles [207]. These folds can be significant, and thus, the forming of multi-layered composites can be challenging to avoid wrinkling. It has been shown that the friction between the plies plays a major role. When simulations of multiply draping are performed with a friction coefficient equal to zero between the layers, the wrinkles do not appear.

Thermoforming of thermoplastic composites

Continuous fibre-reinforced thermoplastics show great potential for large-volume low-cost production of structural components due to low cycle times, material efficiency, and recyclability [211, 212]. Thermoforming processes and related forming defects such as wrinkling are strongly influenced by several processing parameters, e.g., geometry, stacking sequence, tool and initial laminate temperature, press profile, and laminate gripping [213–217]. A virtual analysis and validation of the manufacturability and an optimisation of the involved processing parameters is enabled by macro-scale FE thermoforming simulation, considering material behaviour and processing conditions by constitutive equations and boundary conditions [149]. Moreover, local fibre orientations and forming defects are predictable by a FE forming simulation. The accurate predictions of the forming simulations increase the ability of downstream simulation approaches for their in-service predictions [218, 219]. Due to the growing demand from industry, commercial codes for macroscale FE thermoforming simulation are available and under continuous development [220], such as PAM-FORM [216] and AniForm [54, 221]. LS-DYNA is widely accepted within the US auto industry, and Dassault Systèmes is constantly working to evolve the capabilities of Abaqus where software packages like SimuDrape offer forming-specific add-ons for Abaqus, based e.g. on [94, 166, 190].

Early thermoforming simulation approaches have used homogenisation methods to account for the evolution of the microstructure, by coupling micro-scale unit cell modelling to the macro-scale, to predict the macroscopic forming behaviour [222]. Unit cell modelling is, however, usually applied only to virtual material characterisation [223, 224], while macroscopic approaches are preferred for thermoforming simulation, under the premise to model the evolution of the microstructure in a homogenised manner. Thus, recent thermoforming studies focus on macroscopic approaches.

Experimental characterisations show a distinct rate-dependency of membrane [216, 225–227] and bending behaviour [40, 51, 228]. Consequently, the membrane behaviour of organosheets has been modelled rate-dependent, e.g., through a nonlinear Voigt-Kelvin approach [221], nonlinear hypoelastic approach [229], and Prony series [164]. Dörr et al. [40, 167] compared a nonlinear Voigt-Kelvin and a generalised Maxwell approach to predict the bending and the membrane behaviour of UD tapes. Due to the larger number of model parameters, the generalised Maxwell element showed better agreement with the nonlinear curves from experiments. Several other isothermal approaches are available [230, 231]. However, processing experiments reveal a distinct temperature-dependency [232, 233]. Thus, coupled thermomechanical approaches with temperature-dependent shear and bending have been developed to capture the influence of the transient temperature on the deformation behaviour [229, 234]. A significant modification of the temperature field can be observed during thermoforming. Thus, Guzman-Maldonado et al. [225] developed a thermomechanical approach based on alternating thermal and mechanical simulations. At lower temperatures, the onset of crystallisation may induce a significant increase in mechanical stiffness [233]. Therefore, Dörr et al. [190, 235] developed a coupled thermomechanical approach, considering the phase transition from the molten to the solid material

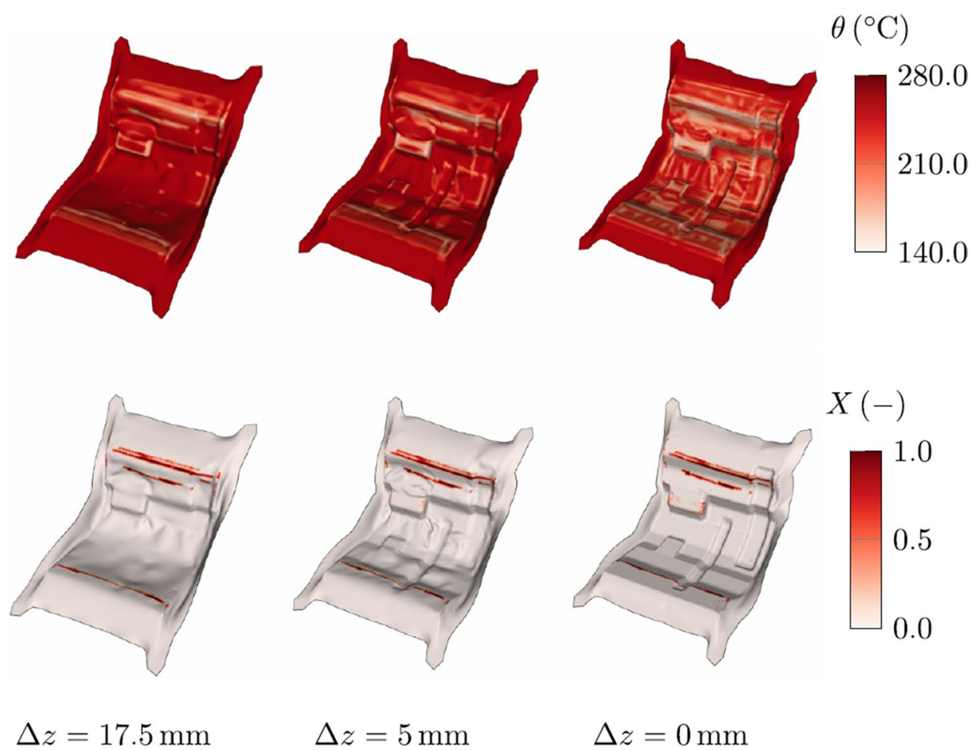

Fig. 10 Thermomechanical forming simulation of an orthotropic layup ($[0;90]_{2\,s}$): Local distribution of Temperature θ and relative crystallinity X at different remaining tool strokes Δz [190]

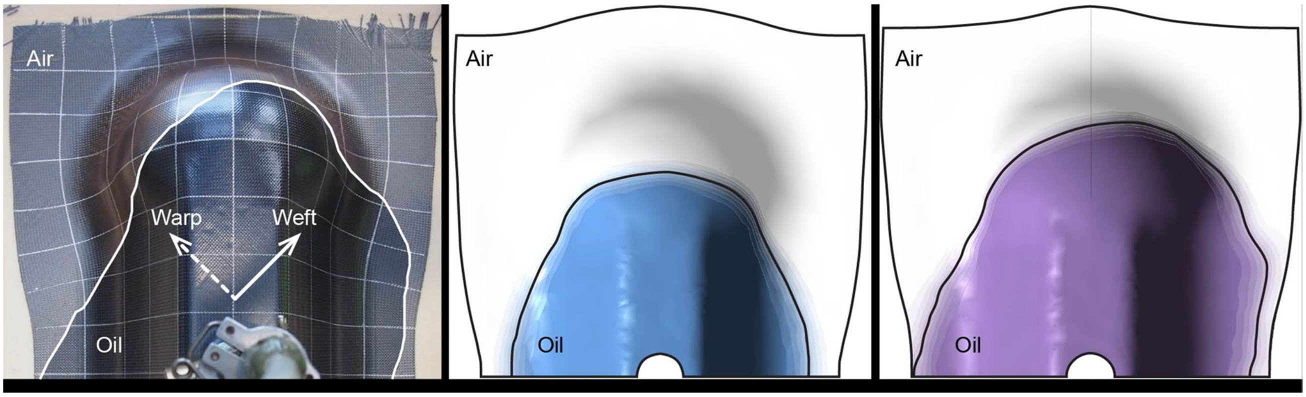

Fig.11 Impregnation of a double-dome mould: (**a**) experiment; (**b**) simulation ignoring and (**c**) simulation accounting for the permeability change caused by the preform deformation [262]

state through crystallisation for semi-crystalline thermoplastics, see Fig. 10. Herein, a modified Nakamura-Ziabicki model is capable to reproduce the crystallization kinetics for the wide range of cooling rates during thermoforming [236]. The contact behaviour between adjacent plies in thermoplastic composites should be modelled as a function of both slip-rate and transversal pressure [221]. For thermomechanical approaches, the dependence on temperature is additionally considered [190]. An investigation of anisotropic inter-ply slip revealed no significant influence of the direction-dependent contact properties on the forming results [237].

Resin infusion, permeability

Permeability

The permeability of a fibrous preform is defined by its internal structure. Therefore, permeability will change as there are changes in the internal structure. Compaction will increase the fibre volume fraction and shear will reduce the spacing between adjacent tows/yarns. Both of these deformation modes will decrease the ability of the resin to flow through the part during forming, and hence decrease the effective permeability.

Local permeability is affected by compaction of the preform, which directly changes the fibre volume fraction. The in-plane permeability phenomenon was studied experimentally in coupled compression-permeability experiments [59, 238] and directly during infusion involving progressive preform compression [239]. Theoretical treatment of the flow/deformation coupling can be found in [240, 241]. The link between compression of the preform and its out-of-plane permeability was studied in [238, 242, 243]; a method of continuous permeability measurement of a preform during compaction was proposed in [244–246].

Shear affects the local permeability principle values: first, because of change of fibre volume fraction of the sheared preform, and also because of change of the details of the internal structure of the fabric. The first cause, change of fibre volume fraction, is much stronger than the second. A simplified estimation of the preform permeability after shear can be done using Kozeny-Carman-type equation with the constants evaluated based on the non-sheared configuration [247–249]. Apart from the change of principal values, the rotation of the permeability must be considered [250]. Permeability of sheared fabrics has been extensively studied experimentally for different types of reinforcement [251–255], including a coupled influence of compaction and shear [256] and effect of shear on dual flow [257]. It was simulated on unit cell models of deformed fabrics [248, 258].

Estimations of the local permeability are coupled with forming simulations, leading to simulations of the part impregnation, which accounts for the local preform structure changes (Fig. 11) [218, 259–262].

The resin flow during the preform impregnation can lead to deformations and distortions of the fibres, as studied by [263, 264].

The permeability research in the last decade was largely shaped by the continuing International Benchmarks. The International Permeability Benchmarks I, II and III on 1D and 2D (radial) permeability measurement methods [265–267] has led to development of an ISO standard for these measurements (this is an ongoing work to be finished in 2022). This work is accompanied by benchmarks on through-the-thickness permeability [241], compressibility of the preforms [70] and virtual permeability [268].

Resin Infusion

Liquid Composite Molding (LCM) is a class of composite manufacturing processes in which a mold cavity containing a reinforcing preform is injected with liquid thermoset resin to fill the empty spaces (pores) between the fibres. LCM processes are versatile and attractive for many industries, such as aerospace, automotive, marine, and civil industries, due to the high volume, the high performance, and the manufacturing of low-cost of polymer composites [269–271]. LCM encompasses several processing options, which can be broadly classified into main groups: (1) matched mold (or rigid mold) processes, such as Resin Transfer Molding (RTM), Compression RTM and Injection Compression Molding, and (2) single-sided mold processes, like Vacuum Assisted Resin Transfer Molding (VARTM), Resin infusion (RI), Seemann's Composite Resin Infusion Molding Process (SCRIMP). Despite the rapid advances in LCM technologies for producing advanced composite parts during the last decade, at present, several unresolved issues persist with respect to process automation, preforming, tooling, mold flow analysis, and resin chemistry. In this regard, significant advancements have been achieved in process modeling and simulation activities [272]. Resin flow through the reinforcement preform is equated to the flow within a porous medium, where the pores between the fibres form interconnected channels. The flow, hence, is described using Darcy's law, which lumps the ease of flow within these channels into a parameter called permeability that characterizes the mobility of the resin through the fibrous porous media [273–275]. Textile permeability, which is an anisotropic and nonhomogeneous property per se, also has a dual-scale nature, being characterized by micron-sized pores that can be individuated within each tow (intra-tow porosity) and millimeter-sized pores between the tows (inter-tow porosity) [276–278]. This inhomogeneity makes it challenging to develop the definition of a reliable model to predict the resin flow behavior. Two methodologies have been investigated to resolve this problem. The first one involves the addition of a sink term in a mesoscale simulation to determine the effective properties of the porous medium and their constitutive equations, and coupling the mesoscopic and macroscopic governing equations [279, 280]. The evaluation of the sink term, which strictly depends on the type, size, and architecture of fabric reinforcement, has been addressed by proposing numerical expression for simplified geometries [276, 281–285] or deriving a formulation considering the actual shape of fabric and tows and the variation in processing conditions by running mesoscopic simulation [279, 286]. The latter involves assessing simultaneously the macro-flow and the micro-flow [284, 287] by using an analytical description [288], semi-empirical expression[289, 290], and numerical tools [277, 278]. Numerical simulation allows one to achieve relevant benefits in the design of the infusion process strategies; however, online monitoring and control of the resin flow and the curing process are still paramount [291]. Indeed, unexpected phenomena during infusion could result in incomplete or nonuniform wetting of the reinforcement, the presence of dry spots and a poor-quality fibre-matrix interface, fibres washing. Each of these defects will have detrimental effects on the mechanical properties of the final part [292–294]. The capability to detect and to correct flow anomalies is critical to a producing high-quality products [295]. Different approaches and sensing devices have been proposed to monitor the resin flow; however, a definitive solution is still yet to be developed. Visual observation by using high-resolution cameras in the case of transparent tooling was proposed by Nielsen and Pitchumani [296] and further developed in automation processing [297]. Tracking and controlling the resin flow through the preform by using pressure sensors embedded in the mold was investigated by Di Fratta et al. [298, 299]. Embedded dielectric sensors were tested by [279, 288, 300] who also claimed low-cost efficiency, sensitivity, and reliability, together with a minimally invasive technique in comparison to other sensor devices. Thermocouples have been used to detect the temperature history of the resin, to evaluate the degree of 02, and to assess the position of the flow-front by looking at the temperature difference between resin and mold; however, limited results have been obtained with metallic molds [301, 302]. Ultrasonic sensors are able to detect the arrival of the resin and evaluate the curing progress by measuring the variations in velocity and attenuation of sound waves [301, 303, 304]. However, some concerns have arisen on the measurement reliability of transducers in industrial operative conditions [305]. Fibre optic sensors represent a noninvasive tool to monitor the manufacturing process: variations in the refractive index of the light beam can be related to the advancing flow or temperature variations during the cure and the material transitions (gel point, glass transition) [306–309]. Their low weight and limited dimensions, on the order of the single fibres, allow them to be embedded within the dry preform without detrimental effect on the structural integrity of the composite part. Resistive sensors consisting of a pair of parallel conductive wires or punctual probes have been successfully used to detect the arrival and curing of the resin by measuring the voltage and variation in conductance of the reference electrical circuit [304, 310, 311]. Issues related to the sensor calibration, to being invasive and to the concern that can be used only once have limited wide acceptance into composite manufacturing. Conductive wires arranged in a grid of line sensors and embedded within the dry perform were proposed by Fink et al. [312, 313] thereby developing the SMARTweave sensor system. The possibility of using conductive fibres (i.e. carbon fibres) as sensing elements reduces the impact of embedded sensors on the in-service integrity and performance of composite parts [314, 315]. X-ray methodology has recently been proposed to visualize the flow pattern and the saturation of the fibre reinforcement [316–318].

Alternative manufacturing processes

Automated fibre placement—Three-dimensional printing

With the introduction and the growing of the concept of Industry 4.0, the fibre-reinforced polymer composite industry is increasing demand for automation on one hand to improve the manufacturing efficiency, while on the other hand production flexibility as the market requires customized products, with specific physical and mechanical properties and complex shapes. These two conflicting needs have pushed the scientific community towards the definition of suitable solutions combining process quality, versatility, and efficiency. Robotic automated processes and three-dimensional printing of continuous-fibre reinforcements are the most reliable responses to these industrial necessities [319]. Both of these classes of processes are based on an additive approach.

Among the robotic/automated processes, the automated fibre placement, automated tape laying and robotic layup are the most relevant manufacturing techniques [320]. These techniques are able to produce high-quality components and are widely adopted by the aeronautic industry [321]. Automated fibre placement is inspired by the filament winding process and consists of the oriented deposition and compaction of pre-impregnated bands of narrow width (up to 15 mm), to form multilayer laminates of complex shapes [322]. The equipment consists of a deposition head capable to start, stop and control the tow flow, to compact the deposited materials, and to cut the filament [323]. The head is mounted on a handling system with at least six degrees of freedom, which make the process capable to manufacture complex shaped surfaces [324]. Automated tape laying is based on the same principle of the automatic fibre placement. In the case of tape laying, the deposited bands of pre-impregnated fibres can be up to 300-mm wide. The large bands and the high average velocity of the a tape-placement system achieve remarkable deposition rates [325]. On the other hand, automated tape laying cannot produce double curvature surfaces and is limited in the manufacturing of small-sized details [325]. Robotic layup consists in the replacement of the human intervention in the operations of fibre reinforcement placement and orientation [326]. In this case, the manufacturing system consists of anthropomorphic robotic arms equipped with multifunction end effectors capable to pick, place, compact and handle dry or pre-impregnated textiles, achieving complex shape and minimizing the presence of defects, such as wrinkles or misorientation [108]. In all of the aforementioned cases, the composite material is deposited or shaped with the support of a mold.

Three-dimensional printing is a widespread additive technique to produce complex shaped elements without the presence of a mold. It is widely applied to process conventional materials, such as polymers. Recently, this technique is being applied to multiphase polymeric based systems [327]. In this context, it is necessary to make a distinction between discontinuous fibre- or particle-reinforced polymers and continuous fibre reinforced polymers. In the case of discontinuous reinforcement systems, the dispersed phase consists typically of short fibres, powders or carbon nanotubes. The phases are combined offline during the filament preparation [328]. The most popular technique to 3D-print continuous-fibre reinforced polymers is fused deposition modeling. In this case, the impregnation can be achieved offline using pre-impregnated filaments online and then combining polymeric filament and continuous-fibre filament in the extruding head [329, 330]. Continuous fibre 3D-printed components are characterized by high anisotropy due to the possibility to orient the fibrous reinforcement as a function of spatial location. A recent advancement of this technique is for 4D printing, in which smart materials (stimuli-responsive, time-dependent, or self-evolving materials) are involved [331].

Wet compression moulding (WCM)

WCM is a closed-mould process with simultaneous draping (forming) and mould-filling (infiltration), which offers strong potential for large-scale production of continuous-fibre reinforced plastics. It has been broadly deployed in the automotive industry within the last ten years, e.g., for structural parts within the car bodies of the BMW i3 and i8 [332, 333]. The key challenge for processing and modelling is the simultaneous multi-physical process with mutual dependency between forming and infiltration [334–338]. Simultaneous infiltration and short infiltration paths allow for relatively low cavity pressures compared to conventional RTM processing [335].

Large deformations during moulding require modelling of textile deformation mechanisms such as membrane, bending and contact behaviours. Comparable to thermoplastic UD tapes or organo sheets, material behaviour is affected by the current infiltration state during modelling [336, 338]. Additionally, fluid redistribution inside the mould requires considering shear-dependent, viscoelastic compaction behaviour [68, 339] as part of a three-dimensional formulation for the draping model [191, 340–342]. In contrast to VARI [343] or RTM injection [288, 344], mould-filling needs to be modelled simultaneously, not sequentially [345] Like other LCM processes, infiltration and flow-front progression are modelled assuming porous media through-flow [346]. Thereby, deformation of the porous medium is considered via local fibre-volume-content (FVC) and fibre orientation (anisotropic flow progression) [247, 254] modelling of deformation and infiltration requires a mutual coupling between an explicitly solved draping model (large interface slip) and a commonly implicitly solved fluid model based on a Stokes, or Darcy flow [343]. The absence of a distinct interface between forming and fluid domains impedes coupling with external codes or the application of CEL methods [347–349]. One solution for a monolithic coupling of draping and infiltration undergoing large strains has been presented by Poppe et al. [342, 345]. Here, a Darcy-based formulation for the fluid model based on an explicit time integration schema is superimposed to an explicitly formulated FE draping model, see Fig. 12. However, further enhancements regarding curing [350] and multi-phase flows [351] are required for accurate WCM modelling.

Process defect: Flow-induced fibre displacements

Fluid injection into the completely-closed (RTM) or partly-closed mould (CRTM) imposes drag forces on the porous medium [352, 353], which can lead to undesired deformation and process defects. Extensively studied for HP-RTM injection, fibre washout and flow-induced fibre-displacement (FiFD) are the two most common defects [354, 355]. While fibre washout relates to the mesoscopic effect of individual rovings being washed out of the textile by high drag forces, FiFD addresses a macroscopic local or global fibre displacement within the stack during infiltration [356]. Modelling requires a strong Fluide Structure interaction (FSI) between material deformation and fluid pressure distribution, often achieved using Terzaghi's effective stress approach [357]. Recently, Hautefeuille et al. [264, 358] demonstrated the high relevance of FiFD for WCM. They demonstrated that the large fibre slip significantly affects the FVC and the resulting pressure distribution. Thus, an accurate prediction of WCM processing forces relies on simultaneous modelling deformation and infiltration. Poppe et al. [359] show that the viscous compaction forces within a porous medium become predictable when a strong FSI is introduced to a suitable WCM process model. Moreover, local deformation depends on the applied contact formulation, as infiltrated regions require a hydrodynamic contact formulation. Further work focuses on superficial fluid and coupled-interface flows [352] as FiFD is often caused by a mix of superficial- and porous-media through-flow.

Pultrusion

Pultrusion is a continuous manufacturing process adopted to produce constant cross-section profiles in fiber reinforced polymer composites. The pultrusion process was designed and patented starting from the half of the twentieth century. The initial target of the process was the production of low performance components, such as fishing rods and lightweight shafts [360]. During the following decades, the performances of the pultruded composites have been dramatically improved through the usage of evolved reinforcing architectures and the better knowledge of the polymerization reaction. Nowadays, pultrusion process is adopted to produce beams and columns widely employed as structural elements in civil buildings, structural supports and decks for bridges, marine piles and constructions, rebars, blades for

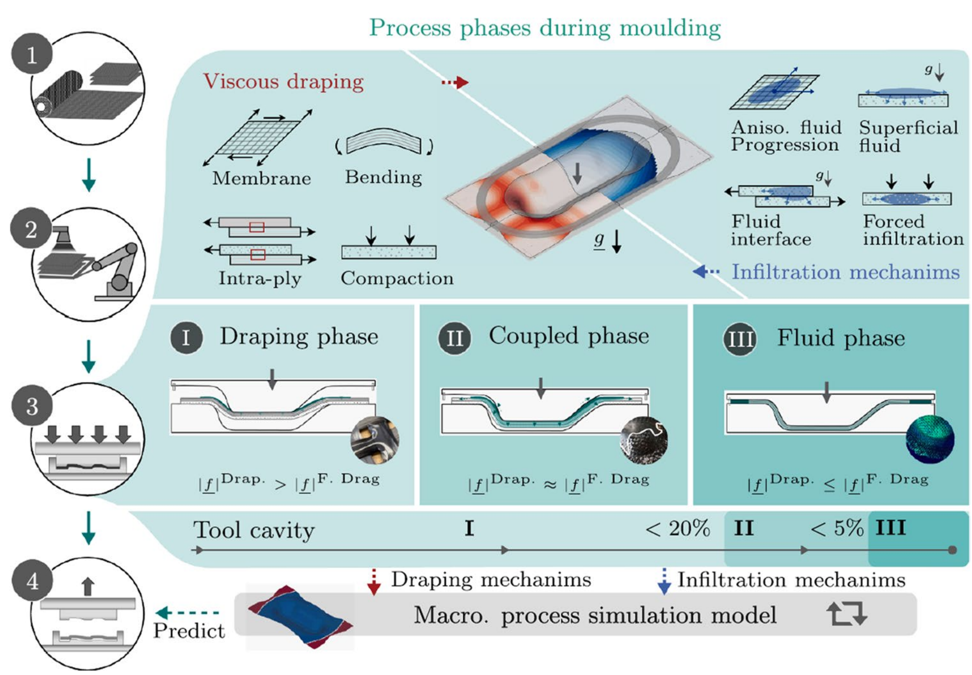

Fig. 12 Process phases and relevant physical mechanisms in Wet Compression Moulding [342]

wind-turbines, structural elements in aircrafts, automotive, and ships [269, 361–364].

Conventional pultrusion is mainly adopted to process thermoset based composites. It consists in forcing the advancement of the fibers through a resin open bath, and then through a heated mold which shapes the composite and activate the cure reaction. Even if most of the industrial pultrusion processes involves thermoset resin systems, starting from '80 s, fiber reinforced thermoplastics have been pultruded as well [365, 366]. Typically, in this case, prepreg tows are employed, to avoid the online impregnation which is more problematic due to the high viscosity of the thermoplastics [367].

The most common variant of the conventional process for fiber reinforced thermosets is the injection pultrusion, whose schematic view is represented in Fig. 13a. This pultrusion variant was first introduced in the early '90 s [368–370]. It avoids the potentially dangerous direct contact between the resin and the surrounding working environment. Indeed, the resin is injected through the dry fiber inside a converging chamber bolted at the die entrance [371, 372].

The process is influenced by different aspects, such as the composition of the resin system or the inhomogeneous distribution of the reinforcing fibers [373, 374]. Several challenging aspects are related to the process planning and control. Fast curing is the main target in pultrusion. Nevertheless, the resin must be catalyzed in such a way to be almost unreactive at room temperature and fully polymerize during the die crossing time. The polymerization of thermosetting systems is a highly exothermal process. Faster reactions determine higher heat flow generations per unit of resin mass, which in turn imply higher thermal loads [375]. The physic state of the resin system is responsible for the interaction between the die cavity walls and the advancing processed materials, and, therefore, for the arising of loads resistant to the pulling forces [376–378].

The thermochemical modeling of pultrusion played a key role in the process development since it allowed the

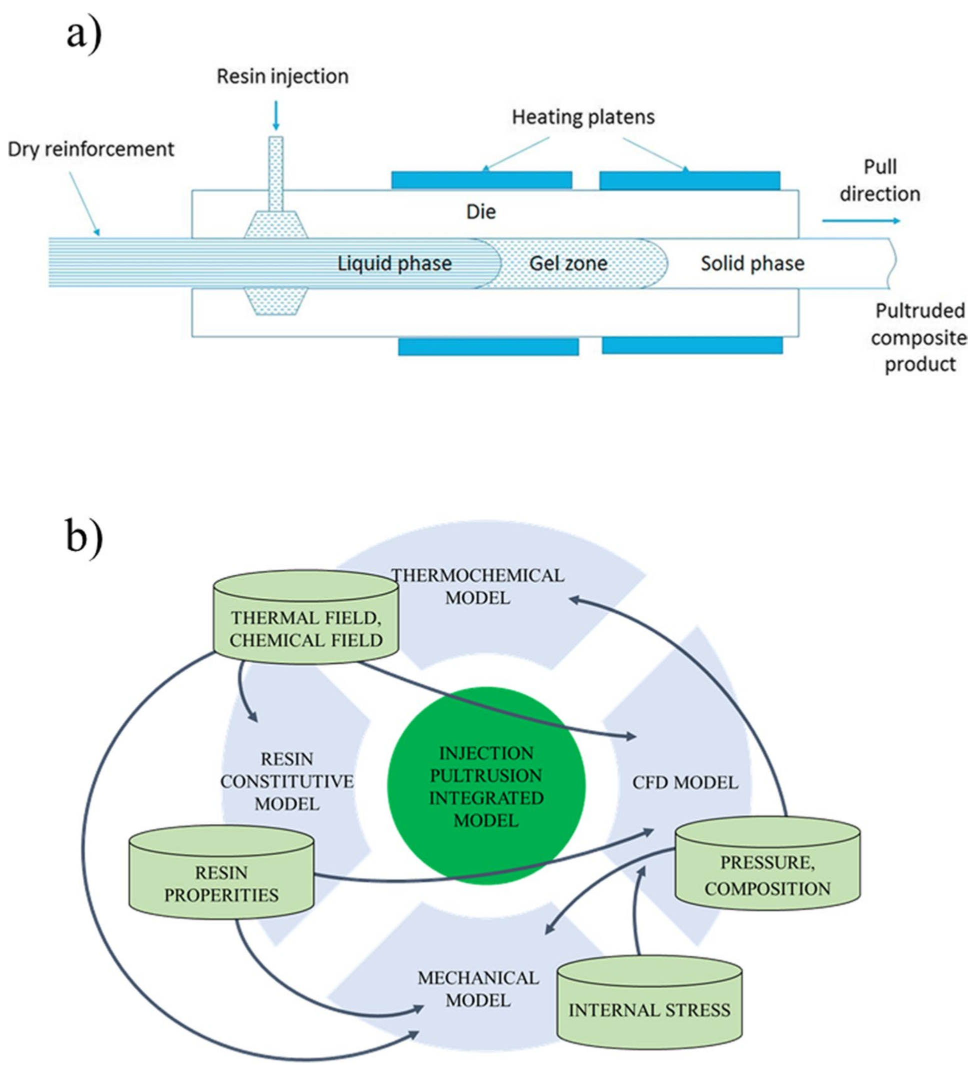

Fig. 13 **a** Schematic view of an injection pultrusion line [399]; **b** schematic view of the physical interconnections in the integrated modeling injection pultrusion

production designer to simulate and predict the capacity of the process to achieve a satisfactory polymerization and to avoid process-related issues such as fast curing or non-homogeneous curing, resin volume shrinkage, thermal expansion/contractions. These effects give place to undesired shape distortions, internal tensions, and crack defects [379–382]. In the late '80 s the thermochemical models proposed were based on one dimensional steady-state heat-transfer [383]. In the successive decades, scientists and researchers developed more sophisticated methods based on two dimensional and three-dimensional heat-transfer, thanks to the increase in the computing power available [384, 385].

Resin flow is another key-aspect in pultrusion. The resin system, while it is in liquid state, flows through the dry fibers and fills the space between them excluding the presence of air. The temperature increase due to the proximity to the heating plates determines a marked decrease of the resin viscosity, promoting in turn the impregnation of the fibrous reinforcement. On the other hand, the thermal energy triggers the cure reaction, which determines a sharp gel-glass transition of the resin. Therefore, a satisfactory impregnation of the fibrous reinforcement must be achieved before the polymerization onset [386].

As well as in the case of the thermochemical behavior, the first computed fluid dynamic models of pultrusion appeared in literature at the end of the '80 s [387]. The effectiveness of the model mostly depends on the good evaluation of the resin rheology, which in turn depends on its thermochemical state [388]. During the following years, some authors developed two-dimensional models of the resin flow in injection pultrusion [389, 390]. Also in this case, the improvement of the computational tools allowed the researchers to develop reliable three-dimensional flow models considering also the presence of a secondary phase, such as air [386].

In this context, in which the behaviors are interconnected and influence each other as described in Fig. 13b, modeling and predicting the pultrusion process performances play a key role [392–396]. The process parameters, namely the platen heating temperatures and the pulling speed, must be carefully ruled and optimized to mitigate the temperature peaks and avoid excessively fast reactions [391, 397–400].

Summary and future outlook

The development of textile-reinforced polymer-matrix composite materials in particular in aerospace and automotive industry has led to many research efforts in the field of composite forming. This field of research is wide because the composite processes are numerous, complex and often new. The physics of deformation during forming is relatively complicated due to the mechanical behaviours of the textile reinforcements and their interaction with the liquid matrix. It has been shown in this article that significant advances have been made in this field in the last 25-plus years. The group of researchers in the field of composite forming is very active within the ESAFORM association. A large part of the research teams in the field took part in the mini-symposium "Composite Forming Processes" and contributed in the discussions in this area. However, the forming processes of composites are numerous and complex, and many advances remain to be made so that the phenomena involved during forming are well understood and accurately modeled. This mini-symposium should be a privileged place to define the directions of future research and also what is needed to increase the adoption speed of models developed here by industry and what areas would require communities to work together. There is considerable research to be conducted to ensure that numerical simulation codes for composite forming processes can be used routinely in the design for manufacturability.

Acknowledgements The authors are grateful to their colleagues, Dr. Dominik Dörr, Dr. Christian Poppe, Bastian Schäfer, Dr. Fausto Tucci, Dr. Felice Rubino, for their support in gathering the relevant literature to make this review paper as complete as possible on the brevity of the pages.

Funding This work has not received any specific funding.

Declarations

Conflict of interests The authors declare that they have no conflict of interest.

References

1. Lindberg J, Behre B, Dahlberg B (1961) Shearing and buckling of various commercial fabrics. Text Res J 31(2):99–122
2. Grosberg P, Park BJ (1966) The mechanical properties of woven fabrics, part V: the initial modulus and the frictional restraint in shearing of plain weave fabrics. Text Res J 36:420–431
3. Kawabata S, Niwa M, Kawai H (1973) 5—The finite-deformation theory of plain-weave fabrics. Part III: The shear-deformation theory. J Textile Institute 64(2):62–85
4. McGuinness GB, OBradaigh CM (1997) Development of rheological models for forming flows and picture-frame shear testing of fabric reinforced thermoplastic sheets. J Non-Newtonian Fluid Mech 73:1–28
5. Wang J, Page JR, Paton R (1998) Experimental investigation of the draping properties of reinforcement fabrics. Compos Sci Technol 58:229–237
6. Lebrun G, Bureau MN, Denault J (2003) Evaluation of biasextension and picture-frame test methods for the measurement of intraply shear properties of PP/glass commingled fabrics. Compos Struct 61:341–352
7. Lomov SV, Verpoest I (2006) Model of shear of woven fabric and parametric description of shear resistance of glass woven reinforcements. Compos Sci Technol 66:919–933

8. Willems A, Lomov SV, Verpoest I, Vandepitte D (2008) Optical strain fields in shear and tensile testing of textile reinforcements. Compos Sci Technol 68(3–4):807–819
9. Cao J, Akkerman R, Boisse P, Chen J et al (2008) Characterization of mechanical behavior of woven fabrics: experimental methods and benchmark results. Compos Part A 39:1037–1053
10. Liu L, Chen J, Li X, Sherwood J (2005) Two-Dimensional Macro-Mechanics Shear Models of Woven Fabrics. Compos A 36(1):105–114
11. Harrison P, Clifford MJ, Long AC (2004) Shear characterisation of viscous woven textile composites, a comparison between picture frame and bias-extension experiments. Compos Sci Technol 64:1453–1465
12. Launay J, Hivet G, Duong AV, Boisse P (2008) Experimental analysis of the influence of tensions on in plane shear behaviour of woven composite reinforcements. Compos Sci Technol 68:506–515
13. Wang P, Hamila N, Pineau P, Boisse P (2014) Thermomechanical analysis of thermoplastic composite prepregs using bias-extension test. J Thermoplast Compos Mater 27(5):679–698
14. White K, Krogh C, Sherwood J (2019) Investigation of Shear Characterization of UHMWPE Unidirectional and Highly-Directional Cross-plies for Finite Element Simulation of Composite Processing, 22nd ESAFORM Conference on Material Forming, Victoria-Gastiez, Spain
15. Krogh C, Dangora L, White K, Jakobsen J, Sherwood J (2019) 256 Shades of Gray: Application of Image Processing to Evaluate the Effect of Sample Geometry and Constant Shear Strain Rates in the Picture-Frame Test, 22nd ESAFORM Conference on Material Forming Victoria-Gastiez, Spain
16. Komeili M, Milani AS (2016) (2016), On effect of shear-tension coupling in forming simulation of woven fabric reinforcements. Compos Part B Eng 99:17–29
17. Yao Y, Peng X, Gong Y (2019) Influence of tension–shear coupling on draping of plain weave fabrics. J Mater Sci 54:6310–6322
18. Alshahrani H. (2020), Characterization and finite element modeling of coupled properties during polymer composites forming processes. Mech Mater;144: 103370
19. Boisse P, Hamila N, Madeo A (2016) Modelling the development of defects during composite reinforcements and prepreg forming. Philosophical Transactions of the Royal Society A: Mathematical, Physical and Engineering Sciences 374(2071):20150269
20. Harrison P, Abdiwi F, Guo Z, Potluri P, Yu WR (2012) Characterising the shear–tension coupling and wrinkling behavior of woven. Compos Part A 43:903–914
21. Nosrat-Nezami F, Gereke T, Eberdt C, Cherif C (2014) Characterisation of the shear–tension coupling of carbon-fibre fabric under controlled membrane tensions for precise simulative predictions of industrial preforming processes. Compos Part A 67:131–139
22. Kashani MH, Rashidi A, Crawford BJ, Milani AS (2016) Analysis of a two-way tension-shear coupling in woven fabrics under combined loading tests: Global to local transformation of non-orthogonal normalized forces and displacements. Compos A 88:272–285
23. Montazerian H, Rashidi A, Hoorfar M, Milani AS (2019) A frameless picture frame test with embedded sensor: Mitigation of imperfections in shear characterization of woven fabrics. Compos Struct 211:112–124
24. Prodromou A, Chen J (1997) On the Relationship between Shear Angle and Wrinkling of Textile Composite Preforms. Compos Part A, Appl Sci Manuf 28:491–503
25. Rozant O, Bourban P-E, Månson J-A (2000) Drapability of Dry Textile Fabrics for Stampable Thermoplastic Preforms. Compos Part A Appl Sci Manuf 31:1167–1177
26. Sharma SB, Sutcliffe MPF, Chang SH (2003) Characterisation of material properties for draping of dry woven composite material. Compos Part A 34:1167–1175
27. Huang J, Boisse P, Hamila N, Gnaba I, Soulat D, Wang P (2021) Experimental and numerical analysis of textile composite draping on a square box. Influence of the weave pattern. Compos Struct 267:113844
28. Boisse P, Hamila N, Guzman-Maldonado E, Madeo A, Hivet G, Dell'Isola F (2017) The bias-extension test for the analysis of in-plane shear properties of textile composite reinforcements and prepregs: a review. IntJ Mater Form 10(4):473–492
29. Peng XQ, Cao J (2005) A continuum mechanics-based non-orthogonal constitutive model for woven composite fabrics. Compos A 36(6):859–874
30. Cao J, Composites Forming, Cao research lab, Northwestern, https://www.cao.mech.northwestern.edu/composites-forming/, Accessed February, 09 2022
31. Boisse P, Cherouat A, Gelin JC, Sabhi H (1995) Experimental study and finite element simulation of a glass fiber fabric shaping process. Polym Compos 16(1):83–95
32. Ten Thije RHW, Akkerman R, Huétink J (2007) Large deformation simulation of anisotropic material using an updated Lagrangian finite element medthod. Comp Meth Appl Mech Engin 196(33–34):3141–3150
33. Dong L, Lekakou C, Bader MG (2001) Processing of composites: simulations of the draping of fabrics with updated material behaviour law. J Compos Mater 35(2):138–163
34. Chen S, Harper LT, Endruweit A, Warrior NA (2015) Formability optimisation of fabric preforms by controlling material draw-in through in-plane constraints. Compos A 76:10–19
35. Boisse P, Hamila N, Vidal-Sallé E, Dumont F (2011) Simulation of wrinkling during textile composite reinforcement forming. Influence of tensile, in-plane shear and bending stiffnesses. Compos Sci Technol 71(5):683–692
36. Liang B, Hamila N, Peillon M, Boisse P (2014) Analysis of thermoplastic prepreg bending stiffness during manufacturing and of its influence on wrinkling simulations. Compos A 67:111–122
37. Dangora LM, Mitchell CJ, Sherwood JA (2015) Predictive model for the detection of out-of-plane defects formed during textile-composite manufacture. Composites Part A 78:102–112
38. Yu F, Chen S, Harper LT, Warrior NA (2021) Simulating the effect of fabric bending stiffness on the wrinkling behaviour of biaxial fabrics during preforming. Composites Part A 143:106308
39. Döbrich O, Gereke T, Diestel O, Krzywinski S, Cherif C (2014) Decoupling the bending behavior and the membrane properties of finite shell elements for a correct description of the mechanical behavior of textiles with a laminate formulation. J Ind Textil 44(1):70–84
40. Dörr D, Schirmaier FJ, Henning F, Kärger L (2017) A viscoelastic approach for modeling bending behavior in finite element forming simulation of continuously fiber reinforced composites. Compos A 94:113–123
41. Peirce FT (1930) The "handle" of cloth as a measurable quantity. J Textil Inst Trans 21(9):T377-416
42. ISO (2011) Reinforcement fabrics — determination of conventional flexural stiffness —fixed-angle flexometer method ISO 4604
43. De Bilbao E, Soulat D, Hivet G, Gasser A (2010) Experimental study of bending behavior of reinforcements. Exp Mech 50(3):333–351
44. Soteropoulos D, Fetfatsidis K, Sherwood J, Langworthy J (2011) Digital Method of Analyzing the Bending Stiffness of

Non-Crimp Fabrics. Proceedings of the 14th ESAForm Conference on Material Forming. April 27–29, 2011. Belfast, Ireland, AIP Conference Proceedings 1353(2011):913
45. Liang B, Chaudet P, Boisse P. Curvature determination in the bending test of continuous fibre reinforcements. Strain 2017;53(1).
46. Kawabata S (1980) The standardization and analysis of hand evaluation. The Textile Machinery Society of Japan, Osaka
47. Lomov SV, Verpoest I, Barburski M, Laperre J (2003) Carbon composites based on multiaxial multiply stitched preforms. Part 2. KES-F characterisation of the deformability of the preforms at low loads. Compos A 34(4):359–70
48. Sachs U, Akkerman R (2017) Viscoelastic bending model for continuous fiber-reinforced thermoplastic composites in melt. Compos A Appl Sci Manuf 100:333–341
49. Wang J, Long AC, Clifford MJ (2010) Experimental measurement and predictive modelling of bending behaviour for viscous unidirectional composite materials. Int J Material Form 3(2):1253–1266
50. Martin TA, Bhattacharyya D, Collins IF (1995) Bending of fibre-reinforced thermoplastic sheets. Compos Manuf 6(34):177–187
51. Margossian A, Bel S, Hinterhoelzl R (2015) Bending characterisation of a molten unidirectional carbon fibre reinforced thermoplastic composite using a Dynamic Mechanical Analysis system. Compos A 77:154–163
52. Alshahrani H, Hojjati M (2017) A new test method for the characterization of the bending of textile prepregs. Compos A 97:128–140
53. Dangora LM, Mitchell C, White KD, Sherwood JA, Parker JC (2018) Characterization of temperature-dependent tensile and flexural rigidities of a cross-ply thermoplastic lamina with implementation into a forming model. IntJ Mater Form 11(1):43–52
54. Haanappel SP, Ten Thije RHW, Sachs U, Rietman B, Akkerman R (2014) Formability analyses of uni-directional and textile reinforced thermoplastics. Compos A 56:80–92
55. Chen B, Colmars J, Naouar N, Boisse P (2021) A hypoelastic stress resultant shell approach for simulations of textile composite reinforcement forming. Composites Part A: Applied Science and Manufacturing 149:106558
56. Boisse P, Colmars J, Hamila N, Naouar N, Steer Q (2018) Bending and wrinkling of composite fiber preforms and prepregs. A review and new developments in the draping simulations. Compos B Eng 141:234–249
57. Robitaille F, Gauvin R (1998) Compaction of textile reinforcements for composites manufacturing. I: Review of experimental results. Polym Compos 19(2):198–216
58. Chen B, Chou T-W (2000) Compaction of woven-fanric preforms: nesting and multi-layer deformation. Compos Sci Technol 60:2223–2231
59. Comas-Cardona S, Le Grognec P, Binetruy C, Krawczak P (2007) Unidirectional compression of fibre reinforcements. Part 1: A non-linear elastic-plastic behaviour. Compos Sci Technol 67(3):507–514
60. Endruweit A, Long AC (2010) Analysis of compressibility and permeability of selected 3d woven reinforcements. J Compos Mater 44(24):2833–2862
61. Lomov SV, Gorbatikh L, Kotanjac Z, Koissin V, Houlle M, Rochez O, Karahan M, Mezzo L, Verpoest I (2011) Compressibility of carbon woven fabric with carbon nanotubes grown on the fibres. Compos Sci Technol 71(3):315–325
62. Lomov SV, Wicks S, Gorbatikh L, Verpoest I, Wardle BL (2014) Compressibility of nanofiber-grafted alumina fabric and yarns: Aligned carbon nanotube forests. Compos Sci Technol 90:57–66
63. Gutowski TG, Kingery J, Boucher D (1986) Experiments in composites consolidation: fiber deformation. Annual Technical Conference of the Society of Plastic Engineers. Brookfield: 1316–1320
64. Lomov SV, Verpoest I (2000) Compression of woven reinforcements: a mathematical model. J Reinf Plast Compos 19(16):1329–1350
65. Chen B, Cheng AH-D, Chou T-W (2001) A nonlinear compaction model for fibrous preforms. Compos A 32:701–707
66. Chen ZR, Ye L (2006) A micromechanical compaction model for woven fabric preforms. Part II: Multilayer. Compos Sci Technol 66(16):3263–3272
67. Chen ZR, Ye L, Kruckenberg T (2006) A micromechanical compaction model for woven fabric preforms. Part I: Single layer. Compos Sci Technol 66(16):3254–3262
68. Bickerton, S., M. J. Buntain and A. A. Somashekar (2003) "The viscoelastic compression behavior of liquid composite molding preforms." Composites Part A, 431–444
69. Kelly PA, Umer R, Bickerton S (2006) Viscoelastic response of dry and wet fibrous materials during infusion processes. Compos A 37(6):868–873
70. Yong AXA, Aktas A, May D, Endruweit A, Lomov SV et al (2020) Experimental characterisation of textile compaction response: a benchmark exercise. Composites Part A 142:106243
71. May D, Kühn F, Etchells M, Fauster E, Endruweit A, Lira C (2019) A reference specimen for compaction tests of fiber reinforcements. Advanced Manufacturing: Polymer & Composites Science 5(4):230–233
72. Sousa P, Lomov SV, Ivens J (2020) Methodology of dry and wet compressibility measurement. Composites Part A 128:105672
73. Werlen V, Rytka C, Michaud V (2021) A numerical approach to characterize the viscoelastic behaviour of fibre beds and to evaluate the influence of strain deviations on viscoelastic parameter extraction. Composites Part a-Applied Science and Manufacturing 143:106315
74. Steer Q, Colmars J, Boisse P (2018) Stitch Modeling of Non Crimp Fabric in Forming Simulations. 21st International ESAFORM Conference on Material Forming (ESAFORM), Univ Palermo, Palermo, ITALY
75. Lomov SV (ed) (2011) Non-crimp fabric composites: manufacturing, properties and applications. Cambridge, Woodhead Publisher Ltd
76. Mikkelsen LP, Fæster S, Goutianos S, Sørensen BF (2021) Scanning electron microscopy datasets for local fibre volume fraction determination in non-crimp glass-fibre reinforced composites. Data in Brief 35:106868
77. Straumit I, Hahn C, Winterstein E, Plank B, Lomov SV, Wevers M (2016) Computation of permeability of a non-crimp carbon textile reinforcement based on X-ray computed tomography images. Compos A 81:289–295
78. Auenhammer RM, Mikkelsen LP, Asp LE, Blinzler BJ (2020) "Dataset of non-crimp fabric reinforced composites for an X-ray computer tomography aided engineering process." Data in Brief 33
79. Auenhammer RM, Mikkelsen LP, Asp LE, Blinzler BJ (2021) Automated X-ray computer tomography segmentation method for finite element analysis of non-crimp fabric reinforced composites. Composite Structures 256:113136
80. Korkiakoski S, Sarlin E, Suihkonen R, Saarela O (2017) Internal structure and fatigue performance of quasi-unidirectional non-crimp fabric reinforced laminates. J Compos Mater 51(24):3405–3423
81. Wilhelmsson D, Gutkin R, Edgren F, Asp LE (2018) An experimental study of fibre waviness and its effects on compressive properties of unidirectional NCF composites. Compos A 107:665–674

82. Kunze E, Galkin S, Bohm R, Gude M, Karger L (2020) The Impact of Draping Effects on the Stiffness and Failure Behavior of Unidirectional Non-Crimp Fabric Fiber Reinforced Composites. Materials 13(13):2959
83. Rouf K, Worswick MJ, Montesano J (2021) A multiscale framework for predicting the mechanical properties of unidirectional non-crimp fabric composites with manufacturing induced defects. J Compos Mater 55(6):741–757
84. Colin D, Bel S, Hans T, Hartmann M, Drechsler K (2020) Virtual Description of Non-Crimp Fabrics at the Scale of Filaments Including Orientation Variability in the Fibrous Layers. Appl Compos Mater 27(4):337–355
85. Bel S, Boisse P, Dumont F (2012) Analyses of the Deformation Mechanisms of Non-Crimp Fabric Composite Reinforcements during Preforming. Appl Compos Mater 19:513–528
86. Schirmaier FJ, Weidenmann KA, Karger L, Henning F (2016) Characterisation of the draping behaviour of unidirectional non-crimp fabrics (UD-NCF). Compos A 80:28–38
87. Christ M, Herrmann A (2018) Definition and quantification of drapeability through the measurement of constituent effects. 13th International Conference on Textile Composites (TEXCOMP), Milan, ITALY
88. Krieger H, Gries T, Stapleton SE (2018) Design of Tailored Non-Crimp Fabrics Based on Stitching Geometry. Appl Compos Mater 25(1):113–127
89. Pourtier J, Duchamp B, Kowalski M, Wang P, Legrand X, Soulat D (2019) Two-way approach for deformation analysis of non-crimp fabrics in uniaxial bias extension tests based on pure and simple shear assumption. IntJ Mater Form 12(6):995–1008
90. Habboush A, Shao HQ, Jiang JH, Chen NL (2020) Characterization and analysis of in-plane shear behavior for glass warp knitted non-crimp fabrics based on bias extension experiment. J Text Inst 111(3):394–404
91. Ghazimoradi M, Trejo EA, Carvelli V, Butcher C, Montesano J (2021) Deformation characteristics and formability of a tricot-stitched carbon fiber unidirectional non-crimp fabric. Composites Part A 145:106366
92. Krishnappa L, Ohlendorf JH, Brink M, Thoben KD (2021) Investigating the factors influencing the shear behaviour of 0/90° non-crimp fabrics to form a reference shear test. J Compos Mater 55(20):2739–2750
93. Avgoulas EI, Mulvihill DM, Endruweit A, Sutcliffe MPF, Warrior NA, De Focatiis DSA, Long AC (2018) Frictional behaviour of non-crimp fabrics (NCFs) in contact with a forming tool. Tribol Int 121:71–77
94. Schirmaier FJ, Dörr D, Henning F et al (2017) A macroscopic approach to simulate the forming behaviour of stitched unidirectional non-crimp fabrics (UD-NCF). Compos A 102:322–335
95. Trejo EA, Ghazimoradi M, Butcher C, Montesano J (2020) Assessing strain fields in unbalanced unidirectional non-crimp fabrics. Composites Part A 130:105758
96. Grieser T, Mitschang P (2017) Investigation of the Compaction Behavior of Carbon Fiber NCF for Continuous Preforming Processes. Polym Compos 38(11):2609–2625
97. Dangora L, Sherwood J, Petrov A, Gorczyca J, Mitchell JG (2013) Forming of Composites using Discontinuous Non-Crimp Fabrics. 28th Technical Conference of the American-Society-for-Composites. Penn State Univ, PA, USA
98. Lin WN, Jiang YM, Qi YX, Qiao CC, Liao QF, Yang C (2020) Study on shearing shrinkage properties of multilayered biaxial weft knitted fabrics. J Textile Inst 112(10):1678–1687
99. Arnold SE, Sutcliffe MPF, Oram WLA (2016) Experimental measurement of wrinkle formation during draping of non-crimp fabric. Compos A 82:159–169
100. Chen S, McGregor OPL, Harper LT, Endruweit A, Warrior NA (2016) Defect formation during preforming of a bi-axial non-crimp fabric with a pillar stitch pattern. Compos A 91:156–167
101. Ali H, Noor S, Shao HQ, Jiang JH, Chen NL (2020) Characterization and analysis of wrinkling behavior of glass warp knitted non-crimp fabrics based on double-dome draping geometry. J Eng Fibers Fabr 15:1558925020958521
102. Kärger L, Galkin S, Kunze E, Gude M, Schäfer B (2021) Prediction of forming effects in UD-NCF by macroscopic forming simulation – Capabilities and limitations. Proceedings ESAFORM 2021. 24th International Conference on Material Forming, Liège, Belgique
103. Mattner T, Wrensch M, Drummer D (2020) Shear behavior of woven and non-crimp fabric based thermoplastic composites at near-processing conditions. Composites Part B 185:107761
104. Christ M, Miene A, Morschel U (2017) Measurement and Analysis of Drapeability Effects of Warp-Knit NCF with a Standardised, Automated Testing Device. Appl Compos Mater 24(4):803–820
105. Mallach A, Hartel F, Heieck F, Fuhr JP, Middendorf P, Gude M (2017) Experimental comparison of a macroscopic draping simulation for dry non-crimp fabric preforming on a complex geometry by means of optical measurement. J Compos Mater 51(16):2363–2375
106. Bardl G, Nocke A, Hubner M, Gereke T, Pooch M, Schulze M, Heuer H, Schiller M, Kupke R, Klein M, Cherif C (2018) Analysis of the 3D draping behavior of carbon fiber non-crimp fabrics with eddy current technique. Compos B 132:49–60
107. Khan AM, Bardl G, Nocke A, Cherif C (2019) Quality analysis of 2D and 3D-draped carbon preforms by eddy current scanning. Composites Part B-Engineering 176:107110
108. Denkena B, Schmidt C, Werner S, Schwittay D (2021) Development of a Shape Replicating Draping Unit for Continuous Layup of Unidirectional Non-Crimp Fabrics on Complex Surface Geometries. J Compos Sci 5:1–13
109. Zhu SQ, Magnussen CJ, Judd EL, Frank MC, Peters FE (2017) "Automated Composite Fabric Layup for Wind Turbine Blades." Journal of Manufacturing Science and Engineering-Transactions of the Asme 139(6)
110. Jagpal R, Butler R, Loukaides EG (2019) Towards flexible and defect-free forming of composites through distributed clamping. 2nd CIRP Conference on Composite Material Parts Manufacturing (CIRP-CCMPM), Univ Sheffield, Adv Mfg Res Ctr, Catcliffe, ENGLAND
111. Krieger H, Gries T, Stapleton SE (2018) Shear and drape behavior of non-crimp fabrics based on stitching geometry. IntJ Mater Form 11(5):593–605
112. Bohler P, Hartel F, Middendorf P (2013) Identification of forming limits for unidirectional carbon textiles in reality and mesoscopic simulation. 16th ESAFORM Conf.on Material Forming. Aveiro, Portugal.
113. Zouari B, Dumont F, Daniel JL, Boisse P (2003) Analyses of woven fabric shearing by optical method and implementation in a finite element program. Proc. 6th ESAFORM Conf. Salerno: 875–887
114. Daniel JL, Soulat D, Boisse P (2004) Shear and tension stiffness influence in composites forming modelling. Proceedings ESAFORM-2004. Trondheim: 301–304
115. Hivet G, Dumont F, Launay J, Maurel V, Vacher P, Boisse P (2004) Optical analysis of woven fabric's shear behaviour. Proceedings ESAFORM-2004. Trondheim: 353–356
116. Lomov SV, Willems A, Barburski M, Stoilova T, Verpoest I (2005) Strain field in the picture frame test: Large and small scale optical measurements. Procedings of the 8th ESAFORM Conference on Material Forming. Cluj-Napoca: 935–938

117. Willems A, Vanderpitte D, Lomov SV, Verpoest I (2005) Biaxial tensile tests on a woven glass/PP fabric under optical strain measurement. Procedings of the 8th ESAFORM Conference on Material Forming. Cluj-Napoca: 1007–1010
118. Lomov SV, Willems A, Verpoest I, Zhu Y, Barburski M, Stoilova T (2006) Picture frame test of woven fabrics with a full-field strain registration. Text Res J 76(3):243–252
119. Zouari B, Daniel JL, Boisse P (2006) A woven reinforcement forming simulation method. Influence of the shear stiffness. Comput Struct 84:651–363
120. Lomov SV, Boisse P, Deluycker E, Morestin F, Vanclooster K, Vandepitte D, Verpoest I, Willems A (2008) Full field strain measurements in textile deformability studies. Compos A 39:1232–1244
121. Zouari R, Amar SB, Dogui A (2010) Experimental and numerical analyses of fabric off-axes tensile test. The Journal of The Textile Institute 101:58–68
122. Zhu B, Yu TX, Tao XM (2007) Large deformation and slippage mechanism of plain woven composite in bias extension. Compos A 38(8):1821–1828
123. Dridi S, Morestin F, Dogui A (2012) Use of digital image correlation to analyse the shearing deformation in woven fabric. Exp Tech 36(5):46–52
124. Khan MA, Mabrouki T, Boisse P (2009) Numerical and experimental forming analysis of woven composites with double dome benchmark. IntJ Mater Form 2:201–204
125. Allaoui S, Boisse P, Chatel S, Hamila N, Hivet G, Soulat D, Vidal-Salle E (2011) Experimental and numerical analyses of textile reinforcement forming of a tetrahedral shape. Compos A 42:612–622
126. Carvelli V, Pazmino J, Lomov SV, Verpoest I (2012) Deformability of a non-crimp 3D orthogonal weave E-glass composite reinforcement. Compos Sci Technol 73:9–18
127. Pazmino J, Carvelli V, Lomov SV (2014) Formability of a non-crimp 3D orthogonal weave E-glass composite reinforcement. Compos A 61:76–83
128. Iwata A, Inoue T, Naouar N, Boisse P, Lomov SV (2019) Coupled meso-macro simulation of woven fabric local deformation during draping. Compos A 118:267–280
129. Eberhardt CN, Clarke AR (2002) Automated reconstruction of curvilinear fibres from 3D datasets acquired by X-ray microtomography. J Microsc 206:41–53
130. Summerscales J, Russell PM, Lomov SV, Verpoest I, Parnas R (2004) The fractal dimension of X-ray tomographic sections of a woven composite. Advanced Composite Letters 13(2):115–123
131. Badel P, Vidal-Salle E, Maire E, Boisse P (2008) Simulation and tomography analysis of textile composite reinforcement deformation at the mesoscopic scale. Compos Sci Technol 68(12):2433–2440
132. Djukic LP, Herszberg I, Schoeppner GA, Brownlow LA (2008) "Tow Visualisation in Woven Composites using X-Ray Computed Tomography." Rec. Adv.in Textile Composites (TexComp-9): 417–425
133. Liu Y, Straumit I, Vasiukov D, Lomov SV, Panier S (2017) Prediction of linear and nonlinear behavior of 3D woven composite using mesoscopic voxel models reconstructed from X-ray microtomography. Compos Struct 179:568–579
134. Graupner N, Beckmann F, Wilde F, Muessig J (2014) Using synchroton radiation-based micro-computer tomography (SR μ-CT) for the measurement of fibre orientations in cellulose fibre-reinforced polylactide (PLA) composites. J Mater Sci 49(1):450–460
135. Naouar N, Vidal-Salle E, Schneider J, Maire E, Boisse P (2014) Meso-scale FE analyses of textile composite reinforcement deformation based on X-ray computed tomography. Compos Struct 116:165–176
136. Pazmino J, Carvelli V, Lomov SV (2014) Micro-CT analysis of the internal deformed geometry of a non-crimp 3D orthogonal weave e-glass composite reinforcement. Compos B 65:147–157
137. Barburski M, Straumit I, Zhang X, Wevers M, Lomov SV (2015) Micro-CT analysis of internal structure of sheared textile composite reinforcement. Compos A 73:45–54
138. Naouar N, Vasiukov D, Park CH, Lomov SV, Boisse P (2020) Meso-FE modelling of textile composites and X-ray tomography. Journal of Material Science 55:16969–16989
139. Naresh K, Khan KA, Umer R, Cantwell WJ (2020) "The use of X-ray computed tomography for design and process modeling of aerospace composites: A review." Mater Des 190
140. Wijaya W, Ali MA, Umer R, Khan KA, Kelly PA, Bickerton S (2019) An automatic methodology to CT-scans of 2D woven textile fabrics to structured finite element and voxel meshes. Composites Part a-Applied Science and Manufacturing 125:105561
141. Wijaya W, Kelly PA, Bickerton S (2020) A novel methodology to construct periodic multi-layer 2D woven unit cells with random nesting configurations directly from mu CT-scans. Composites Science and Technology 193:108125
142. Mendoza A, Trullo R, Wielhorski Y (2021) Descriptive modeling of textiles using FE simulations and deep learning. Composites Science and Technology 213:108897
143. Vidal-Salle E, Nguyen QT, Charmetant A, Breard J, Maire E, Boisse P (2010) Use of numerical simulation of woven reinforcement forming at mesoscale: Influence of transverse compression on the global response. IntJ Mater Form 3:699–702
144. Madra A, Causse P, Trochu F, Adrie J, Maire E, Breitkopf P (2019) Stochastic characterization of textile reinforcements in composites based on X-ray microtomographic scans. Compos Struct 224:111031
145. Vanaerschot A, Cox BN, Lomov SV, Vandepitte D (2016) Experimentally validated stochastic geometry description for textile composite reinforcements. Compos Sci Technol 122:122–129
146. Vanaerschot A, Cox BN, Lomov SV, Vandepitte D (2016) Multiscale modelling strategy for textile composites based on stochastic reinforcement geometry. Comput Methods Appl Mech Eng 310:906–934
147. Straumit I, Lomov SV, Wevers M (2015) Quantification of the internal structure and automatic generation of voxel models of textile composites from X-ray computed tomography data. Compos A 69:150–158
148. Karamov R, Martulli LM, Kerschbaum M, Sergeichev I, Swolfs Y, Lomov SV (2019) Micro-CT based structure tensor analysis of fibre orientation in random fibre composites versus high-fidelity fibre identification methods. Composite Structures 235:111818
149. Kärger L, Galkin S, Dörr D, Poppe C (2020) Capabilities of Macroscopic Forming Simulation for Large-Scale Forming Processes of Dry and Impregnated Textiles. Procedia Manufacturing 47:140–147
150. Xiao H, Bruhns OT, Meyers A (1997) (1997) Hypo-elasticity model based upon the logarithmic stress rate. J Elast 47:51–68
151. Boisse P (2007) Finite element analysis of composite forming. In composites forming technologies, Woodhead publishing, pp.46–79, 2007
152. Xue P, Peng X, Cao J (2003) A non-orthogonal constitutive model for characterizing woven composites. Compos A 34(2):183–193
153. Peng X, Ding F (2011) Validation of a non-orthogonal constitutive model for woven composite fabrics via hemispherical stamping simulation. Compos A 42(4):400–407
154. Yu WR, Harrison P, Long A (2005) Finite element forming simulation for non-crimp fabrics using a non-orthogonal constitutive equation. Compos A 36(8):1079–1093
155. Boisse P, Aimène Y, Dogui A, Dridi S, Gatouillat S, Hamila N, ..., Vidal-Sallé E (2010) Hypoelastic, hyperelastic, discrete and

semi-discrete approaches for textile composite reinforcement forming. Int J Mater Form 3(2):1229-1240
156. Khan MA, Mabrouki T, Vidal-Salle E, Boisse P (2010) Numerical and experimental analyses of woven composite reinforcement forming using a hypoelastic behaviour. Application to the double dome benchmark. J Mater Process Technol 210:378–388
157. Boehler J-P (1987) Applications of Tensor Functions in Solid Mechanics; Springer: Berlin/Heidelberg, Germany; Volume 292
158. Itskov M (2000) On the theory of fourth-order tensors and their applications in computational mechanics. Comput Methods Appl Mech Eng 189(2):419–438
159. Criscione JC, Douglas AS, Hunter WC (2001) Physically based strain invariant set for materials exhibiting transversely isotropic behaviour. J Mech Phys Solids 49:871–897
160. Charmetant A, Orliac JG, Vidal-Sallé E, Boisse P (2012) Hyperelastic model for large deformation analyses of 3D interlock composite preforms. Compos Sci Technol 72(12):1352–1360
161. Pazmino J, Mathieu S, Carvelli V, Boisse P, Lomov SV (2015) Numerical modelling of forming of a non-crimp 3D orthogonal weave E-glass composite reinforcement. Compos A 72:207–218
162. Khiêm VN, Krieger H, Itskov M, Gries T, Stapleton SE (2018) An averaging based hyperelastic modeling and experimental analysis of non-crimp fabrics. Int J of Solids and Structures 154:43–54
163. Holzapfel GA, Gasser TC (2001) A viscoelastic model for fiber-reinforced composites at finite strains: Continuum basis, computational aspects and applications. Comput Methods Appl Mech Eng 190(34):4379–4403
164. Guzman-Maldonado E, Hamila N, Boisse P, Bikard J (2015) Thermomechanical analysis, modelling and simulation of the forming of pre-impregnated thermoplastics composites. Compos A 78:211–222
165. Belnoue JH, Nixon-Pearson OJ, Ivanov D, Hallett SR (2016) A novel hyper-viscoelastic model for consolidation of toughened prepregs under processing conditions. Mech Mater 97:118–134
166. Dörr D, Schirmaier FJ, Henning F, Kärger L (2017) On the relevance of modeling viscoelastic bending behavior in finite element forming simulation of continuously fiber reinforced thermoplastics. In AIP Conference Proceedings 1896(1):030003
167. Dörr D, Henning F, Kärger L (2018) Nonlinear hyperviscoelastic modelling of intra-ply deformation behaviour in finite element forming simulation of continuously fibre-reinforced thermoplastics. Compos A 109:585–596
168. Abdiwi F, Harrison P, Yu WR (2013) Modelling the shear-tension coupling of woven engineering fabrics. Adv Mater Sci Eng 2013:786769
169. Ferretti M, Madeo A, Dell'Isola F, Boisse P (2014) Modeling the onset of shear boundary layers in fibrous composite reinforcements by second-gradient theory. Zeit.t Ange.Math.und Physik, 65(3), 587–612
170. Boisse P, Hamila N, Madeo A (2018) The difficulties in modeling the mechanical behavior of textile composite reinforcements with standard continuum mechanics of Cauchy. Some possible remedies. Int J Solids Struct 154:55–65
171. Mathieu S, Hamila N, Bouillon F, Boisse P (2015) Enhanced modeling of 3D composite preform deformations taking into account local fiber bending stiffness. Compo Sci Technol 117:322–333
172. Madeo A, Ferretti M, Dell'Isola F, Boisse P (2015) Thick fibrous composite reinforcements behave as special second-gradient materials: three-point bending of 3D interlocks. Z Angew Math Phys 66(4):2041–2060
173. Dell'Isola F, Steigmann D (2015) A two-dimensional gradient-elasticity theory for woven fabrics. J Elast 118(1):113–125
174. Dell'Isola F, Cuomo M, Greco L, Della Corte A (2017) Bias extension test for pantographic sheets: numerical simulations based on second gradient shear energies. J Engin Mathematics 103(1):127–157
175. Barbagallo G, Madeo A, Morestin F, Boisse P (2017) Modelling the deep drawing of a 3D woven fabric with a second gradient model. Math Mech Solids 22(11):2165–2179
176. Steer Q, Colmars J, Naouar N, Boisse P (2021) Modeling and analysis of in-plane bending in fibrous reinforcements with rotation-free shell finite elements. Int. J. of Solids and Structures 222:111014
177. Billoet JL, Cherouat A (2001) Mechanical and numerical modelling of composite manufacturing processes deep-drawing and laying-up of thin pre-impregnated woven fabrics. J Mater Process Technol 118:460–471
178. Lee JS, Hong SJ, Yu W-R et al (2007) The effect of blank holder force on the stamp forming behavior of non-crimp fabric with a chain stitch. Compos Sci Technol 67:357–366
179. Lin H, Wang J, Long AC et al (2007) Predictive modelling for optimization of textile composite forming. Compos Sci Technol 67:3242–3252
180. Skordos AA, Monroy Aceves C, Sutcliffe MPF (2007) A simplified rate dependent model of forming and wrinkling of pre-impregnated woven composites. Compos A 38:1318–1330
181. Jauffrès D, Sherwood J, Morris C, Chen J (2009) Discrete Mesoscopic Modeling for the Simulation of Woven-Fabric Reinforcement Forming. Int Journal of Forming 3:1205–1216
182. Soulat D, Cheruet A, Boisse P (2006) Simulation of continuous fibre reinforced thermoplastic forming using a shell finite element with transverse stress. Comput Struct 84:888–903
183. Hamila N, Boisse P, Sabourin F et al (2009) A semi-discrete shell finite element for textile composite reinforcement forming simulation. Int J Numer Meth Engng 79:1443–1466
184. Liang B, Colmars J, Boisse P (2017) A shell formulation for fibrous reinforcement forming simulations. Compos A 100:81–96
185. Wang P, Hamila N, Boisse P (2013) Thermoforming simulation of multilayer composites with continuous fibres and thermoplastic matrix. Compos B Eng 52:127–136
186. Wang P, Legrand X, Boisse P, Hamila N, Soulat D (2015) Experimental and numerical analyses of manufacturing process of a composite square box part: Comparison between textile reinforcement forming and surface 3D weaving. Compos B Eng 78:26–34
187. Chen B, Boisse P, Colmars J, Naouar N, Bai R, Chaudet P (2021) Analysis of the Forming of Interlock Textile Composites Using a Hypoelastic Approach. Applied Composite Materials, 1–16
188. Bel S, Hamila N, Boisse P, Dumont F (2012) Finite element model for NCF composite reinforcement preforming: Importance of inter-ply sliding. Compos A 43(12):2269–2277
189. Hübner M, Rocher J-E, Allaoui S et al (2016) Simulation-based investigations on the drape behavior of 3D woven fabrics made of commingled yarns. Int J Mater Form 9:591–599
190. Dörr D, Joppich T, Kugele D et al (2019) A coupled thermomechanical approach for finite element forming simulation of continuously fiber-reinforced semi-crystalline thermoplastics. Composites Part A 125:105508
191. Bai Renzi, Colmars Julien, Naouar Naim, Boisse Philippe (2020) A specific 3D shell approach for textile composite reinforcements under large deformation. Composites A 139:106135
192. Bai R, Colmars J, Chen B, Naouar N, Boisse P (2022) The fibrous shell approach for the simulation of composite draping with a relevant orientation of the normals. Composite Structures 115202
193. Ahmad S, Irons BM, Zienkiewicz OC (1970) Analysis of thick and thin shell structures by curved finite elements. Int J Numer Meth Eng 2(3):419–451

194. Schäfer B, Dörr D, Kärger L (2020) Reduced-Integrated 8-Node Hexahedral Solid-Shell Element for the Macroscopic Forming Simulation of Continuous Fibre-Reinforced Polymers. Proc Manufactur 47:134–139
195. Chen QQ, Saouab A, Boisse P et al (2009) Woven thermoplastic composite forming simulation with solid-shell element method. Int J Simul Multidisci Des Optim 3:337–341
196. Xiong H, Guzman Maldonado E, Hamila N et al (2018) A prismatic solid-shell finite element based on a DKT approach with efficient calculation of through the thickness deformation. Finite Elem Anal Des 151:18–33
197. Schäfer B, Dörr D, Kärger L (2021) Potential and challenges of a solid-shell element for the macroscopic forming simulation of engineering textiles. ESAFORM 2021
198. Zhu B, Yu TX, Teng J, Tao XM (2009) Theoretical Modeling of Large Shear Deformation and Wrinkling of Plain Woven Composite. J Compos Mater 43:125–138
199. Lightfoot JS, Wisnom MR, Potter K (2013) Defects in woven preforms: formation mechanisms and the effects of laminate design and layup protocol. Composites A 51:99–107
200. Bloom LD, Wang J, Potter KD (2013) Damage Progression and Defect Sensitivity: An Experimental Study of Representative Wrinkles in Tension. Compos Part B Eng 45:449–458
201. Lightfoot JS, Wisnom MR, Potter K (2013) A New Mechanism for the Formation of Ply Wrinkles Due to Shear between Plies. Compos Part A 49:139–147
202. Sjölander J, Hallander P, Åkermo M (2016) Forming Induced Wrinkling of Composite Laminates: A Numerical Study on Wrinkling Mechanisms. Compos Part A 81:41–51
203. Belnoue J-H, Nixon-Pearson OJ, Thompson AJ, Ivanov DS, Potter KD, Hallett SR (2018) Consolidation-Driven Defect Generation in Thick Composite Parts. J Manuf Sci Eng 140:071006
204. Cao J, Boyce MC (1997) Wrinkling Behavior of Rectangular Plates under Lateral Constraint. Int J Solids Struct 34:153–176
205. Friedl N, Rammerstorfer FG, Fischer FD (2000) Buckling of Stretched Strips. Comput Struct 78:185–190
206. Huebner M, Diestel O, Sennewald C, Gereke T, Cherif C (2012) Simulation of the Drapability of Textile Semi-Finished Prod-ucts with Gradient-Drapability Characteristics by Varying the Fabric Weave. Fibres & Textiles in Eastern Europe, 20, 5(94): 88–93
207. Guzman-Maldonado E, Wang P, Hamila N, Boisse P (2019) Experimental and Numerical Analysis of Wrinkling during Forming of Multi-Layered Textile Composites. Compos Struct 208:213–223
208. Vanclooster K, Lomov SV, Verpoest I (2009) On the formability of multi-layered fabric composites, In: ICCM—17th Int. Conf. on Composite Materials, Edinburgh, UK
209. Vanclooster K, Lomov SV, Verpoest I (2010) Simulation of Multi-Layered Composites Forming. IntJ Mater Form 3:695–698
210. Ten Thije R, Akkerman R (2009) A Multi-Layer Triangular Membrane Finite Element for the Forming Simulation of Laminated Composites. Compos A 40:739–753
211. Friedrich K, Almajid AA (2013) Manufacturing aspects of advanced polymer composites for automotive applications. Appl Compos Mater 20(2):107–128
212. Henning F, Kärger L, Dörr D, Schirmaier FJ, Seuffert J, Bernath A (2019) Fast processing and continuous simulation of automotive structural composite components. Compos Sci Technol 171:261–279
213. Joppich T, Doerr D, van der Meulen L, Link T, Hangs B, Henning F (2016) Layup and process dependent wrinkling behavior of PPS/CF UD tape-laminates during nonisothermal press forming into a complex component. AIP Conf Proc 1769:170011
214. Boisse P (2015) editor. Advances in composites manufacturing and process design. Woodhead publishing series in composites science and engineering, Vol. 56. Cambridge UK: Woodhead Publishing
215. Schug A, Winkelbauer J, Hinterhölzl R, Drechsler K (2017) Thermoforming of glass fibre reinforced polypropylene: A study on the influence of different process parameters. In AIP Conference Proceedings 1896(1):030010
216. de Luca P, Lefébure P, Pickett AK (1998) Numerical and experimental investigation of some press forming parameters of two fibre reinforced thermoplastics: APC2-AS4 and PEI-CETEX. Compos Part A 29(1–2):101–110
217. Benkaddour A, Lebrun G, Laberge-Lebel L (2017) Thermostamping of [0/90]n carbon/peek laminates: influence of support configuration and demolding temperature on part consolidation. Polym Compos 22:42
218. Kärger L, Bernath A, Fritz F, Galkin S, Magagnato D, Oeckerath A, Schön A, Henning F (2015) Development and validation of a CAE chain for unidirectional fibre reinforced composite components. Compos Struct 132:350–358
219. Kärger L, Galkin S, Zimmerling C, Dörr D, Linden J, Oeckerath A, Wolf A (2018) Forming optimisation embedded in a CAE chain to assess and enhance the structural performance of composite components. Compos Struct 192:143–152
220. Dörr D, Brymerski W, Ropers S, Leutz D, Joppich T, Kärger L, Henning F (2017) A Benchmark Study of Finite Element Codes for Forming Simulation of Thermoplastic UD-Tapes. Special Issue Procedia CIRP 66:101–106
221. Haanappel S (2013) Forming of UD fibre reinforced thermoplastics: a critical evaluation of intra-ply shear PhD thesis Enschede, the Netherlands: Universiteit Twente
222. Hsiao S-W, Kikuchi N (1999) Numerical analysis and optimal design of composite thermoforming process. Comput Methods Appl Mech Eng 177(1–2):1–34
223. Boisse P, Gasser A, Hagege B, Billoet J-L (2005) Analysis of the mechanical behavior of woven fibrous material using virtual tests at the unit cell level. J Mater Sci 40(22):5955–5962
224. Lin H, Long AC, Sherburn M, Clifford MJ (2008) Modelling of mechanical behaviour for woven fabrics under combined loading. Int J Mater Form 1(1):899–902
225. Guzman-Maldonado E, Hamila N, Naouar N, Moulin G, Boisse P (2016) Simulation of thermoplastic prepreg thermoforming based on a visco-hyperelastic model and a thermal homogenization. Mater Des 93:431–442
226. Machado M, Fischlschweiger M, Major Z (2016) A rate-dependent nonorthogonal constitutive model for describing shear behaviour of woven reinforced thermoplastic composites. Compos A 80:194–203
227. Haanappel SP, Akkerman R (2014) Shear characterisation of unidirectional 550 fibre reinforced thermoplastic melts by means of torsion. Compos A 56:8–26
228. Sachs (2014) Friction and bending in thermoplastic composites forming processes, Phd thesis, Universiteit Twente, Twente, Enschede, The Netheralands
229. Machado M, Murenu L, Fischlschweiger M, Major Z (2016) Analysis of the thermomechanical shear behaviour of woven-reinforced thermoplastic-matrix composites during forming. Compos Part A 86:39–48
230. Gong Y, Peng X, Yao Y, Guo Z (2016) An anisotropic hyperelastic constitutive model for thermoplastic woven composite prepregs. Compos Sci Technol 128:17–24
231. Harrison P, Gomes R, Curado-Correia N (2013) Press forming a 0/90 cross-ply advanced thermoplastic composite using the double-dome benchmark geometry. Compos Part A 54:56–69
232. Ropers S (2017) Bending behavior of thermoplastic composite sheets: viscoelasticity and temperature dependency in the draping process. AutoUni - Schriftenreihe Vol. 99. Wiesbaden and s.l.: Springer Fachmedien Wiesbaden

233. Donderwinkel TG, Rietman B, Haanappel SP, Akkerman R (2016) Stamp forming optimization for formability and crystallinity. AIP Conf Proc 1769:170029
234. Ropers S, Kardos M, Osswald TA (2016) A thermo-viscoelastic approach for the characterization and modeling of the bending behavior of thermoplastic composites. Compos A 90:22–32
235. Dörr D (2019) Simulation of the thermoforming process of UD fiber-reinforced thermoplastic tape laminates. Doctoral thesis, Karlsruhe Institute of Technology (KIT), KITopen, Karlsruhe
236. Kugele D, Dörr D, Wittemann F, Hangs B, Rausch J, Kärger L, Henning F (2017) Modeling of the non-isothermal crystallization kinetics of polyamide 6 composites during thermoforming. AIP Conf Proc. 1869. p. 030005. 20th ESAFORM, Dublin
237. Dörr D, Faisst M, Joppich T, Poppe C, Henning F, Kärger L (2018) Modelling Approach for Anisotropic Inter-Ply Slippage in Finite Element Forming Simulation of Thermoplastic UD-Tapes, AIP Conference Proceedings 1960: 020005, ESAFORM 2018, Palermo
238. George A, Hannibal P, Morgan M, Hoagland D, Stapleton SE (2019) Compressibility measurement of composite reinforcements for flow simulation of vacuum infusion. Polym Compos 40(3):961–973
239. Hoagland D, George A (2017) Continuous permeability measurement during unidirectional vacuum infusion processing. J Reinf Plast Compos 36(22):1618–1628
240. Merotte J, Simacek P, Advani SG (2010) Flow analysis during compression of partially impregnated fiber preform under controlled force. Compos Sci Technol 70(5):725–733
241. Gangloff JJ, Simacek P, Sinha S, Advani SG (2014) A process model for the compaction and saturation of partially impregnated thermoset prepreg tapes. Compos A 64:234–244
242. Endruweit A, Luthy T, Ermanni P (2002) Investigation of the influence of textile compression on the out-of-plane permeability of a bidirectional glass fibre fabric. Polym Compos 23(4):538–554
243. Yong AXH, Aktas A, May D, Endruweit A, Advani S et al (2021) Out-of-plane permeability measurement for reinforcement textiles: A benchmark exercise. Composites Part A 148:106480
244. Ouagne P, Breard J (2010) Continuous transverse permeability of fibrous media. Compos A 41:22–28
245. Ouagne P, Ouahbi T, Park CH, Breard J, Saouab A (2013) Continuous measurement of fiber reinforcement permeability in the thickness direction: Experimental technique and validation. Compos B 45(1):609–618
246. Kabachi MA, Stettler L, Arreguin S, Ermanni P (2021) Concurrent characterization of through-thickness permeability and compaction of fiber reinforcements. Composites Part A 141:106203
247. Demaria C, Ruiz E, Trochu F (2007) In-plane anisotropic permeability characterization of deformed woven fabrics by unidirectional injection. Part II: Prediction model and numerical simulations. Polym Compos 28(6):812–827
248. Verleye B, Croce R, Griebel M, Klitz M, Lomov SV, Morren G, Sol H, Verpoest I, Roose D (2008) Permeability of textile reinforcements: Simulation, influence of shear and validation. Compos Sci Technol 68(13):2804–2810
249. Chen ZM, Pan SD, Zhou ZG, Lei T, Dong BF, Xu PF (2019) The effect of shear deformation on permeability of 2.5d woven preform. Materials 12(21):3594
250. Endruweit A, Ermanni P (2004) The in-plane permeability of sheared textiles. Experimental observations and a predictive conversion model. Compos A 35:439–451
251. Hammami A, Trochu F, Gauvin R, Wirth S (1996) Directional permeability measurement of deformed reinforcement. J Reinf Plast Compos 15(6):552–562
252. Lai C-L, Young W-B (1997) Permeability of fibre reinforcements after shear deformation. Proceedings of ICCM-11. Gold Coast, Australia. IV: 227–236
253. Heardman E, Lecakou C, Bader MG (2001) In-plane permeability of sheared fabrics. Compos A 32:933–940
254. Liotier PJ, Govignon Q, Swery E, Drapier S, Bickerton S (2015) Characterisation of woven flax fibres reinforcements: Effect of the shear on the in-plane permeability. J of Composite Materials 49(27):3415–3430
255. Pierce RS, Falzon BG, Thompson MC (2018) Permeability characterization of sheared carbon fiber textile preform. Polym Compos 39(7):2287–2298
256. Aranda S, Berg DC, Dickert M, Drechsel M, Ziegmann G (2014) Influence of shear on the permeability tensor and compaction behaviour of a non-crimp fabric. Compos B 65:158–163
257. Walther J, Simacek P, Advani SG (2012) The effect of fabric and fiber tow shear on dual scale flow and fiber bundle saturation during liquid molding of textile composites. Int J of Material Forming 5(1):83–97
258. Zeng XS, Endruweit A, Brown LP, Long AC (2015) Numerical prediction of in-plane permeability for multilayer woven fabrics with manufacture-induced deformation. Compos A 77:266–327
259. Slade J, Sozer EM, Advani SG (2000) Fluid impregnation of deformed preforms. J Reinf Plast Compos 19(7):552–568
260. Loix F, Badel P, Orgeas L, Geindreau C, Boisse P (2008) Woven fabric permeability: From textile deformation to fluid flow mesoscale simulations. Compos Sci Technol 68(7–8):1624–1630
261. Pierce RS, Falzon BG (2017) Simulating Resin Infusion through Textile Reinforcement Materials for the Manufacture of Complex Composite Structures. Engineering 3(5):596–607
262. Pierce RS, Falzon BG, Thompson MC (2017) A multi-physics process model for simulating the manufacture of resin-infused composite aerostructures. Compos Sci Technol 149:269–279
263. Klunker F, Danzi M, Ermanni P (2015) Fiber deformation as a result of fluid injection: modeling and validation in the case of saturated permeability measurements in through thickness direction. J Compos Mater 49(9):1091–1105
264. Hautefeuille A, Comas-Cardona S, Binetruy C (2019) Mechanical signature and full-field measurement of flow-induced large in-plane deformation of fibrous reinforcements in composite processing. Compos A 118:213–222
265. Arbter R, Binetruy C, Bizet L, Bréard J et al (2011) Experimental determination of the permeability of textiles: A benchmark exercise. Compos A 42(9):1157–1168
266. Vernet N, Ruiz E, Advani S, Alms JB et al (2014) Experimental determination of the permeability of engineering textiles: Benchmark II. Compos A 61:172–184
267. May D, Aktas A, Advani SG, Berg DC et al (2019) In-plane permeability characterization of engineering textiles based on radial flow experiments: A benchmark exercise. Compos A 121:100–114
268. May D, Syerko E, Schmidt T, Binetruy C, Rocha da Silva L, Lomov SV, Advani S (2021) Benchmarking virtual permeability predictions of real fibrous microstructure. 36th ASC Tech. VIRTUAL Conf.: 2123 - 2132
269. Rubino F, Nisticò A, Tucci F, Carlone P (2020) Marine Application of Fiber Reinforced Composites: A Review. J Mar Sci Eng 8:26
270. Bodaghi M, Lomov SV, Simacek P, Correia NC, Advani SG (2019) On the Variability of Permeability Induced by Reinforcement Distortions and Dual Scale Flow in Liquid Composite Moulding: A Review. Compos Part A 120:188–210
271. Hindersmann A (2019) Confusion about Infusion: An Overview of Infusion Processes. Compos. Part A 126:105583

272. Carlone P, Aleksendrić D (2015) Soft Computing in the Design and Manufacturing of Composite Materials; ISBN 9781782421795.
273. Binétruy C, Hilaire B, Pabiot J (1997) The Interactions between Flows Occurring inside and Outside Fabric Tows during RTM. Compos Sci Technol 57(5):587–596
274. Binetruy C, Hilaire B, Pabiot J (1998) Tow Impregnation Model and Void Formation Mechanisms during RTM. J Compos Mater 32:223–245
275. Pillai KM, Advani SG (1998) A Model for Unsaturated Flow in Woven Fiber Preforms during Mold Filling in Resin Transfer Molding. J Compos Mater 32:1753–1783
276. Parnas RS, Phelan FR (1991) The Effect of Heterogeneous Porous Media on Mold Filling in Resin Transfer Molding. J. Chem. Inf. Model
277. DeParseval Y, Pillai KM, Advani SG (1997) A Simple Model for the Variation of Permeability Due to Partial Saturation in Dual Scale Porous Media. Transp Porous Media 27:243–264
278. Kuentzer N, Simacek P, Advani SG, Walsh S (2006) Permeability Characterization of Dual Scale Fibrous Porous Media. Compos Part A 37:2057–2068
279. Carlone P, Rubino F, Paradiso V, Tucci F (2018) Multi-Scale Modeling and Online Monitoring of Resin Flow through Dual-Scale Textiles in Liquid Composite Molding Processes. Int J Adv Manuf Technol 96:2215–2230
280. Yeager M, Simacek P, Advani SG (2017) Role of Fiber Distribution and Air Evacuation Time on Capillary Driven Flow into Fiber Tows. Compos Part A 93:144–152
281. Pillai KM (2002) Governing Equations for Unsaturated Flow through Woven Fiber Mats. Part 1. Isothermal Flows. Compos Part A 33:1007–1019
282. Zhou F, Kuentzer N, Simacek P, Advani SG, Walsh S (2006) Analytic Characterization of the Permeability of Dual-Scale Fibrous Porous Media. Compos Sci Technol 66:2795–2803
283. Zhou F, Alms J, Advani SG (2008) A Closed Form Solution for Flow in Dual Scale Fibrous Porous Media under Constant Injection Pressure Conditions. Compos Sci Technol 68:699–708
284. Pillai KM, Advani SG (1998) Numerical Simulation of Unsaturated Flow in Woven Fiber Preforms during the Resin Transfer Molding Process. Polym Compos 19:71–80
285. Carlone P, Palazzo GS (2014) Unsaturated and Saturated Flow Front Tracking in Liquid Composite Molding Processes Using Dielectric Sensors. Appl Compos Mater 22:543–557
286. Imbert M, Comas-Cardona S, Abisset-Chavanne E, Prono D (2019) Introduction of Intra-Tow Release/Storage Mechanisms in Reactive Dual-Scale Flow Numerical Simulations. J Compos Mater 53:125–140
287. Michaud V, Mortensen A (2001) Infiltration Processing of Fibre Reinforced Composites: Governing Phenomena. Compos Part A Appl Sci Manuf 32:981–996
288. Michaud V (2016) A Review of Non-Saturated Resin Flow in Liquid Composite Moulding Processes. Transp Porous Media 115:581–601
289. Gascón L, García JA, Lebel F, Ruiz E, Trochu F (2015) Numerical Prediction of Saturation in Dual Scale Fibrous Reinforcements during Liquid Composite Molding. Compos. Part A 77
290. Markicevic B, Djilali N (2006) Two-Scale Modeling in Porous Media: Relative Permeability Predictions. Phys. Fluids 18(3):033101
291. Modi D, Correia N, Johnson M, Long A, Rudd C, Robitaille F (2007) Active Control of the Vacuum Infusion Process. Compos Part A 38:1271–1287
292. Mesogitis TS, Skordos AA, Long AC (2014) Uncertainty in the Manufacturing of Fibrous Thermosetting Composites: A Review. Compos Part A 57:67–75
293. Park CH, Lee W (2011) Modeling Void Formation and Unsaturated Flow in Liquid Composite Molding Processes: A Survey and Review. J Reinf Plast Compos 30:957–977
294. Varna J, Joffe R, Berglund LA, Lundström TS (1995) Effect of Voids on Failure Mechanisms in RTM Laminates. Compos Sci Technol 53:241–249
295. Grossing H, Stadlmajer N, Fauster E, Fleischmann M, Schledjewski R (2016) Flow Front Advancement during Composite Processing: Predictions from Numerical Filling Simulation Tools in Comparison with Real-World Experiments. Polym Compos 37:2782–2793
296. Nielsen DR, Pitchumani R (2002) Control of Flow in Resin Transfer Molding with Real-Time Preform Permeability Estimation. Polym Compos 23:1087–1110
297. Lekanidis S, Vosniakos GC (2020) Machine Vision Support of VARI Process Automation in Composite Part Manufacturing. Int J Mechatronics Manuf Syst 13:169
298. Di Fratta C, Koutsoukis G, Klunker F, Ermanni P (2016) Fast Method to Monitor the Flow Front and Control Injection Parameters in Resin Transfer Molding Using Pressure Sensors. J Compos Mater 50:2941–2957
299. Di Fratta C, Klunker F, Ermanni P (2013) A Methodology for Flow-Front Estimation in LCM Processes Based on Pressure Sensors. Compos Part A 47:1–11
300. Rubino F, Paradiso V, Carlone P (2017) Flow Monitoring of Microwave Pre-Heated Resin in LCM Processes. In Proceedings of the AIP Conference Proceedings; Vol. 1896, p. 030017
301. Tuncol G, Danisman M, Kaynar A, Sozer EM (2007) Constraints on Monitoring Resin Flow in the Resin Transfer Molding (RTM) Process by Using Thermocouple Sensors. Compos Part A 38:1363–1386
302. Wang P, Molimard J, Drapier S, Vautrin A, Minni JC (2012) Monitoring the Resin Infusion Manufacturing Process under Industrial Environment Using Distributed Sensors. J Compos Mater 46:691–706
303. Schmachtenberg E, Schulte Zur Heide J, Töpker J (2005) Application of Ultrasonics for the Process Control of Resin Transfer Moulding (RTM). Polym Test 24:330–338
304. Danisman M, Tuncol G, Kaynar A, Sozer EM (2007) Monitoring of Resin Flow in the Resin Transfer Molding (RTM) Process Using Point-Voltage Sensors. Compos Sci Technol 67:367–379
305. Liebers N, Raddatz F, Schadow F (2016) Effective and flexible ultrasound sensors for cure monitoring for industrial composite production Nico Liebers , Florian Raddatz , Florian Schadow German Aerospace Centre (DLR), Institute of Composite Structures and Adaptive
306. Konstantopoulos S, Fauster E, Schledjewski R (2014) Monitoring the Production of FRP Composites: A Review of in-Line Sensing Methods. Express Polym Lett 8:823–840
307. Khoun L, De Oliveira R, Michaud V, Hubert P (2011) Investigation of Process-Induced Strains Development by Fibre Bragg Grating Sensors in Resin Transfer Moulded Composites. Compos Part A 42:274–282
308. Matsuzaki R, Kobayashi S, Todoroki A, Mizutani Y (2011) Full-Field Monitoring of Resin Flow Using an Area-Sensor Array in a VaRTM Process. Compos Part A 42:550–559
309. Molimard J, Vacher S, Vautrin A (2011) Monitoring LCM Process by FBG Sensor under Birefringence. Strain 47:364–373
310. Lawrence JM, Hsiao KT, Don RC, Simacek P, Estrada G, Sozer EM, Stadtfeld HC, Advani SG (2002) An Approach to Couple Mold Design and On-Line Control to Manufacture Complex Composite Parts by Resin Transfer Molding. Compos - Part A 33:981–990
311. Barooah P, Berker B, Sun JQ (2003) Lineal Sensors for Liquid Injection Molding of Advanced Composite Materials 1–29

312. Fink BK, Gillespie JW, Walsh S, DeSchepper DC, McCullough RL, Don RC (1995) Advances in Resin Transfer Molding Flow Monitoring Using SMARTweave Sensors. Proceedings of ASME, int. mechanical engineering congress and exposition. San Francisco, CA; pp. 999–1015
313. Bradley JE, Diaz-Perez J, Gillespie Jr, JW, Fink BK (1998) On-Line Process Monitoring and Analysis of Large Thick-Section Composite Parts Utilizing SMARTweave in-Situ Sensing Technology. Int. SAMPE Symp. Exhib. 43
314. Vaidya UK, Jadhav NC, Hosur MV, Gillespie JW, Fink BK (2000) Assessment of Flow and Cure Monitoring Using Direct Current and Alternating Current Sensing in Vacuum-Assisted Resin Transfer Molding. Smart Mater Struct 9:727–736
315. Dominauskas A, Heider D, Gillespie JW (2003) Electric Time-Domain Reflectometry Sensor for Online Flow Sensing in Liquid Composite Molding Processing. Compos Part A 34:67–74
316. Teixidó H, Caglar B, Revol V, Michaud V (2021) In-Operando Dynamic Visualization of Flow through Porous Preforms Based on X-Ray Phase Contrast Imaging. Compos. Part A 149:106560
317. Larson NM, Zok FW (2018) Insights from In-Situ X-Ray Computed Tomography during Axial Impregnation of Unidirectional Fiber Beds. Compos Part A 107:124–134
318. Larson NM, Cuellar C, Zok FW (2019) X-Ray Computed Tomography of Microstructure Evolution during Matrix Impregnation and Curing in Unidirectional Fiber Beds. Compos Part A 117:243–259
319. Parmar H, Khan T, Tucci F et al (2021) Advanced robotics and additive manufacturing of composites: towards a new era in Industry 4.0. Mater. Manuf. Process. 1–35
320. Frketic J, Dickens T, Ramakrishnan S (2017) Automated manufacturing and processing of fiber-reinforced polymer (FRP) composites: An additive review of contemporary and modern techniques for advanced materials manufacturing. Addit Manuf 14:69–86
321. Grant C (2006) Automated processes for composite aircraft structure. Ind Rob 33:117–121
322. Vernejoux C, Fischer X, Deseur S (2021) Duc E (2021) Influence of Automated Fiber Placement Parameters on Thermoplastic Composite Blanks Used on Stamp Forming Process. ESAFORM 02:1–11
323. Debout P, Chanal H, Duc E (2011) Tool path smoothing of a redundant machine: Application to Automated Fiber Placement. CAD Comput Aided Des 43:122–132
324. Liu Y-N, Yuan C, Liu C et al (2019) Study on the resin infusion process based on automated fiber placement fabricated dry fiber preform. Sci Rep 9:7440
325. Crosky A, Grant C, Kelly D et al (2015) Fibre placement processes for composites manufacture. In: Advances in Composites Manufacturing and Process Design. Elsevier, pp 79–92
326. Esperto V, Gambardella A, Pasquino G et al (2021) (2021) Modeling and Simulation of the Robotic Layup of Fibrous Preforms for Liquid Composite Molding. ESAFORM 02:1–10
327. Parandoush P, Lin D (2017) A review on additive manufacturing of polymer-fiber composites. Compos Struct 182:36–53
328. Sánchez DM, de la Mata M, Delgado FJ et al (2020) Development of carbon fiber acrylonitrile styrene acrylate composite for large format additive manufacturing. Mater Des 191:108577
329. Chacón JM, Caminero MA, Núñez PJ et al (2019) Additive manufacturing of continuous fibre reinforced thermoplastic composites using fused deposition modelling: Effect of process parameters on mechanical properties. Compos Sci Technol 181:107688
330. Chang B, Li X, Parandoush P et al (2020) Additive manufacturing of continuous carbon fiber reinforced poly-ether-ether-ketone with ultrahigh mechanical properties. Polym Test 88:106563
331. Rafiee M, Farahani RD, Therriault D (2020) Multi-Material 3D and 4D Printing: A Survey. Adv Sci 7:1–26
332. Bergmann J, Dormann H, Lange R (2016) Interpreting process data of wet pressing process Part. 1. Theoretical approach. Journal of Composite Materials 50(17):2399–2407
333. Stanglmaier, Stefan Josef (2017) Empirische Charakterisierung und Modellierung des Imprägnierprozesses lokal verstärkter Kohlenstofffaserhalbzeuge im RTM- und Nasspress-Verfahren für die Großserie.
334. Bergmann J, Dormann H, Lange R (2016) Interpreting process data of wet pressing process. Part 2. Verification with real values. In Journal of Composite Materials 50(17):2409–2419
335. Bockelmann P (2017) Process Control in Compression Molding of Composites. Dissertation. München
336. Poppe C, Dörr D, Henning F, Kärger L (2018) Experimental and numerical investigation of the shear behaviour of infiltrated woven fabrics. In Composites Part A 114:327–337
337. Albrecht, Fabian; Poppe, Christian; Fial, Julian; Rosenberg, Philipp; Middendorf, Peter; Henning, Frank (Eds.) (2020) Impact of process routing on part infiltration during wet compression moulding (WCM). With assistance of Fabian Albrecht, Christian Poppe, Julian Fial, Philipp Rosenberg, Peter Middendorf, Frank Henning. Sampe Europa. Amsterdam
338. Poppe Christian, Rosenkranz Tobias, Dörr Dominik, Kärger Luise (2019) Comparative experimental and numerical analysis of bending behaviour of dry and low viscous infiltrated woven fabrics. Composites Part A 124:105466
339. Ivanov DS, Lomov SV (2014) Compaction behaviour of dense sheared woven preforms. Experimental observations and analytical predictions. Composites Part A 64:167–176
340. Boisse P, Bai R, Colmars J, Hamila N, Liang B, Madeo A (2018) The Need to Use Generalized Continuum Mechanics to Model 3D Textile Composite Forming. Appl Compos Mater 25(4):761–771
341. Xiong Hu, Hamila N, Boisse P (2019) Consolidation Modeling during Thermoforming of Thermoplastic Composite Prepregs. Materials 12(18):2853
342. Poppe Christian T, Krauß Constantin, Albrecht Fabian, Kärger Luise (2021) A 3D process simulation model for wet compression moulding. Composites Part A 145:106379
343. Dereims A, Drapier S, Bergheau J-M, de Luca P (2015) 3D robust iterative coupling of Stokes, Darcy and solid mechanics for low permeability media undergoing finite strains. In Fini Elem Anal Des 94:1–15
344. Rudd, Long, Kendall, Mangin (1997) Liquid moulding technologies. Resin transfer moulding, structural reaction injection moulding and related processing techniques. With assistance of C. D. Rudd. Cambridge: Woodhead.
345. Poppe, Christian; Dörr, Dominik; Henning, Frank; Kärger, Luise (2018) A 2D modeling approach for fluid propagation during FE-forming simulation of continuously reinforced composites in wet compression moulding. In. Proceedings of the 21st international esaform conference on material forming: ESAFORM 2018. Palermo, Italy, 23–25 April 2018 (AIP Conference Proceedings), p. 20022.
346. Correia NC, Robitaille F, Long AC, Rudd CD, Šimáček P, Advani SG (2004) Use of Resin Transfer Molding Simulation to Predict Flow, Saturation, and Compaction in the VARTM Process. J Fluids Eng 126(2):210

347. Celle, Pierre; Drapier, Sylvain; Bergheau, Jean-Michel (2008) Numerical aspects of fluid infusion inside a compressible porous medium undergoing large strain. In *Rev. europ. de méc. num.* 17 (5–6–7), pp. 819–827
348. Celle P, Drapier S, Bergheau J-M (2008) Numerical modelling of liquid infusion into fibrous media undergoing compaction. European Journal of Mechanics - A/Solids 27(4):647–661
349. Pillai KM, Tucker CL, Phelan FR (2001) Numerical simulation of injection/compression liquid composite molding. Part 2. Preform compression. Composites Part A 32(2):207–220
350. Tan H, Pillai KM (2012) Multiscale modeling of unsaturated flow in dual-scale fiber preforms of liquid composite molding III. Reactive flows. Composites Part A 43(1):29–44
351. Seuffert J, Kärger L, Henning F (2018) Simulating Mold Filling in Compression Resin Transfer Molding (CRTM) Using a Three-Dimensional Finite-Volume Formulation. Journal of Composites Science 2(2):23
352. Engmann J, Servais C, Burbidge AS (2005) Squeeze flow theory and applications to rheometry: A review. In Journal of Non-Newtonian Fluid Mechanics 132(1–3):1–27
353. Tucker C, Dessenberger R (1994) Governing equations for flow and heat transfer in stationary fiber beds. In Flow and Rheology in Polymer Composites Manufacturing, pp. 237–257
354. Bodaghi Masoud, Simacek Pavel, Advani Suresh G, Correia Nuno C (2018) A model for fibre washout during high injection pressure resin transfer moulding. J Reinf Plastics and Composites 37(13):865–876
355. Bodaghi M, Simacek P, Correia N, Advani SG (2020) Experimental parametric study of flow-induced fiber washout during high-injection-pressure resin transfer molding. Polymer Composites 41(3):1053–1065
356. Seong DG, Kim S, Um MK, Song YS (2018) Flow-induced deformation of unidirectional carbon fiber preform during the mold filling stage in liquid composite molding process. J Compos Mater 52(9):1265–1277
357. MacMinn Christopher W, Dufresne Eric R, Wettlaufer John S (2016) Large Deformations of a Soft Porous Material. Phys Rev Applied. 5(4):044020
358. Hautefeuille A, Comas-Cardona S, Binetruy C (2020) Consolidation and compression of deformable impregnated fibrous reinforcements: Experimental study and modeling of flow-induced deformations. In Composites Part A 131:105768
359. Poppe, Christian; Albrecht, Fabian; Krauß, Constantin; Kärger, Luise (2021) Towards numerical prediction of flow-induced fiber displacements during wet compression molding (WCM). In *ESAFORM 2021*.
360. Howald AM, Meyer LS. Shaft for fishing rods. US2571717, 1951.
361. Vedernikov A, Safonov A, Tucci F, Carlone P, Akhatov I (2020) Pultruded materials and structures: A review. J Compos Mater 54:4081–4117
362. Ducoulombier N, Demont L, Chateau C, Bornert M, Caron JF (2020) Additive manufacturing of anisotropic concrete: A flow-based pultrusion of continuous fibers in a cementitious matrix. Procedia Manuf 47:1070–1077
363. Baran I, Tutum CC, Hattel JH (2013) The internal stress evaluation of pultruded blades for a darrieus wind turbine. Key Eng Mater 554–557:2127–2137
364. Tucci F, Vedernikov A (2021) Design Criteria for Pultruded Structural Elements. Encycl. Mater. Compos., Elsevier Ltd, p. 51–68
365. Cowen G, Measuria U, Turner RM. (1986) Section pultrusions of continuous fibre reinforced thermoplastics. I Mech E Conf. Publ. Institution Mech. Eng, p. 105–12
366. Offringa A (1988) Design and application of a pultrusion for multiple use in the Fokker 100. Compos Struct 10:199–209
367. Minchenkov K, Vedernikov A, Safonov A, Akhatov I (2021) Thermoplastic pultrusion: A review Polymers (Basel) 13:1–36
368. Kim YR, McCarthy SP, Fanucci JP (1991) Study of resin flow during injection-pultrusion process. Annu. Tech. Conf. - ANTEC, Conf. Proc., vol. 37, p. 1966–9
369. Cho B-G, McCarthy SP, Fanucci JP, Nolet SC (1992) Performance of nylon-6 composites produced by the reaction injection pultrusion process. Int SAMPE Electron Conf 24:645–659
370. Becker H, Fischer G, Muller U (1993) Push-pull injection moulding of industrial products. Kunststoffe, Ger Plast 83:3–4
371. Strauß S, Boysen S, Senz A, Wilhelm F, Rilli N (2021) Analysis of the mechanical composite properties of ii-chamber variations in the closed injection pultrusion process. Esaform 2021(02):1–13. https://doi.org/10.25518/esaform21.970
372. Strauß S (2020) Development of a flexible injection and impregnation chamber for pultrusion of high reactive resins. Procedia Manuf 47:956–961
373. Nasonov Y, Safonov A, Gusev S, Akhatov I (2020) Effect of additives on cure kinetics of pultrusion resins. Procedia Manuf 47:920–924
374. Baran I (2017) Analysis of the local fiber volume fraction variation in pultrusion process. AIP Conf Proc 1896(1):030029
375. Tucci F, Rubino F, Paradiso V, Carlone P, Valente R (2017) Modelling and simulation of cure in pultrusion processes. AIP Conf Proc 1896(1):070003
376. Carlone P, Palazzo GS (2008) Viscous pull force evaluation in the pultrusion process by a finite element thermo-chemical rheological model. Int J Mater Form 1:831–834
377. Baran I, Carlone P, Hattel JH, Palazzo GS, Akkerman R (2014) The effect of product size on the pulling force in pultrusion. Key Eng Mater 611–612:1763–1770
378. Tucci F, Esperto V, Rubino F, Carlone P (2020) Experimental measurement of the resistant load in injection pultrusion processes. Procedia Manuf 47:148–153
379. Tucci F, Rubino F, Carlone P (2018) Strain and temperature measurement in pultrusion processes by fiber Bragg grating sensors. AIP Conf Proc; 1960
380. Yuksel O, Baran I, Ersoy N, Akkerman R (2018) Analysis of residual transverse stresses in a thick UD glass/polyester pultruded profile using hole drilling with strain gage and digital image correlation. AIP Conf Proc 1960
381. Baran I, Hattel JH, Akkerman R (2014) Investigation of the spring-in of a pultruded l-shaped profile for various processing conditions and thicknesses. Key Eng Mater 611–612:273–279
382. Baran I, Hattel JH, Akkerman R (2014) The effect of mandrel configuration on the warpage in pultrusion of rectangular hollow profiles. Key Eng Mater 611–612:250–256
383. Hackett RM, Prasad SN (1989) Pultrusion process modeling. In: Newaz GM, editor. Adv. Thermoplast. Matrix Compos. Mater. (3rd edn.), Philadelphia: ASTM STP 1044, American Society for Testing and Materials, Philadelphia, Pennsylvania, 62–70.
384. Batch GL, Macosko CW (1993) Heat transfer and cure in pultrusion: Model and experimental verification. AIChE J 39:1228–1241
385. Carlone P, Palazzo GS, Pasquino R (2006) Pultrusion manufacturing process development by computational modelling and methods. Math Comput Model 44:701–709

386. Tucci F, Bezerra R, Rubino F, Carlone P (2020) Multiphase flow simulation in injection pultrusion with variable properties. Mater Manuf Process 35:152–162
387. Sumerak JE (1985) Understanding Pultrusion Process Variables. Mod Plast 62
388. Shanku R, Vaughan JG, Roux JA (1997) Rheological characteristics and cure kinetics of EPON 862/W epoxy used in pultrusion. Adv Polym Technol 16:297–311
389. Jeswani AL, Roux JA (2008) Modeling of processing for slot and discrete port tapered resin injection pultrusion. J Thermophys Heat Transf 22:749–757
390. Rahatekar SS, Roux JA (2003) Numerical simulation of pressure variation and resin flow in injection pultrusion. J Compos Mater 37:1067–1082
391. Safonov AA, Carlone P, Akhatov I (2018) Mathematical simulation of pultrusion processes: A review. Compos Struct 184:153–177
392. Tucci F, Rubino F, Esperto V, Carlone P (2019) Integrated modeling of injection pultrusion. AIP Conf. Proc. 2113(1):060006
393. Carlone P, Rubino F, Palazzo GS (2016) Thermo-chemical, mechanical and resin flow integrated analysis in pultrusion. AIP Conf Proc 1769
394. Sandberg M, Rasmussen FS, Hattel JH, Spangenberg J (2019) Simulation of resin-impregnation, heat-transfer and cure in a resin-injection pultrusion process. AIP Conf Proc 2113
395. Carlone P, Baran I, Akkerman R, Palazzo GS (2015) Computational analysis of the interaction between impregnation, forming and curing in pultrusion. Key Eng Mater 651–653:889–894
396. Vedernikov A, Safonov A, Tucci F, Carlone P, Akhatov I (2021) Modeling Spring-In of L-Shaped Structural Profiles Pultruded at Different Pulling Speeds. Polymers 13
397. Tutum CC, Baran I, Hattel JH (2013) Utilizing multiple objectives for the optimization of the pultrusion process based on a thermo-chemical simulation. Key Eng Mater 554–557:2165–2174
398. Vedernikov A, Tucci F, Safonov A, Carlone P, Gusev S, Akhatov I (2020) Investigation on the shape distortions of pultruded profiles at different pulling speed. Procedia Manuf 47:1–5
399. Vedernikov A, Tucci F, Carlone P, Gusev S, Konev S, Firsov D et al (2021) Effects of pulling speed on structural performance of L-shaped pultruded profiles. Compos Struct 255:112967
400. Vedernikov A, Safonov A, Tucci F, Carlone P, Akhatov I (2021) Analysis of Spring-in Deformation in L-shaped Profiles Pultruded at Different Pulling Speeds: Mathematical Simulation and Experimental Results. ESAFORM 2021:1–10